Development/Plasticity/Repair

Heterogeneity and Bipotency of Astroglial-Like Cerebellar Progenitors along the Interneuron and Glial Lineages

Elena Parmigiani,[1,2] Ketty Leto,[1,2] Chiara Rolando,[1,2] María Figueres-Oñate,[3] Laura López-Mascaraque,[3] Annalisa Buffo,[1,2] and Ferdinando Rossi[1,2]†

[1]Department of Neuroscience Rita Levi-Montalcini and Neuroscience Institute Cavalieri Ottolenghi, University of Turin, I-10126 Turin, Italy, [2]Neuroscience Institute Cavalieri Ottolenghi, I-10043 Orbassano, Turin, Italy, and [3]Department of Molecular, Cellular, and Developmental Neurobiology, Cajal Institute, Spanish National Research Council, E-28002 Madrid, Spain

Cerebellar GABAergic interneurons in mouse comprise multiple subsets of morphologically and neurochemically distinct phenotypes located at strategic nodes of cerebellar local circuits. These cells are produced by common progenitors deriving from the ventricular epithelium during embryogenesis and from the prospective white matter (PWM) during postnatal development. However, it is not clear whether these progenitors are also shared by other cerebellar lineages and whether germinative sites different from the PWM originate inhibitory interneurons. Indeed, the postnatal cerebellum hosts another germinal site along the Purkinje cell layer (PCL), in which Bergmann glia are generated up to first the postnatal weeks, which was proposed to be neurogenic. Both PCL and PWM comprise precursors displaying traits of juvenile astroglia and neural stem cell markers. First, we examine the proliferative and fate potential of these niches, showing that different proliferative dynamics regulate progenitor amplification at these sites. In addition, PCL and PWM differ in the generated progeny. GABAergic interneurons are produced exclusively by PWM astroglial-like progenitors, whereas PCL precursors produce only astrocytes. Finally, through *in vitro*, *ex vivo*, and *in vivo* clonal analyses we provide evidence that the postnatal PWM hosts a bipotent progenitor that gives rise to both interneurons and white matter astrocytes.

Key words: **Bergmann glia; cerebellum; mouse brain; multipotent progenitors; neurogenesis; prospective white matter**

Introduction

The anatomic complexity of the cerebellum originates embryonically from the epithelium of the fourth ventricle [ventricular zone (VZ)] and the anterior rhombic lip (RL). In these germinal niches, progenitors with astroglial features [bona fide radial glia (RG); Mori et al., 2006] give rise to all the glutamatergic and GABAergic cerebellar neurons, respectively (Carletti and Rossi, 2008). Interestingly, cerebellar development continues after birth, when secondary proliferative sites replace the embryonic niches. Postnatally, proliferative progenitors reside in the external granular layer (EGL), in the prospective white matter (PWM), and along the Purkinje cell layer (PCL; Altman and Bayer, 1997). Although the EGL exclusively produces granule neurons (Hallonet et al., 1990; Alvarez-Otero et al., 1993), the PWM comprises cells belonging to the interneuronal, astroglial, and oligodendroglial lineages (Leto et al., 2012). The PCL instead hosts a subset of postmitotic Bergmann glia (BG) and precursors for this astroglial type (Yamada and Watanabe, 2002; Sudarov et al., 2011; Buffo and Rossi, 2013). However, a neurogenic potential has also been hypothesized for PCL-residing progenitors (Alcock et al., 2007; Alcock and Sottile 2009).

Notably, progenitors in both PCL and PWM display similar traits of immature astroglia and prospective neural stem cell (NSC) markers (Yamada and Watanabe, 2002; Anthony et al., 2004; Lee et al., 2005; Alcock et al., 2007; Alcock and Sottile, 2009; Silbereis et al., 2009; Fleming et al., 2013). Beside these similarities, the specific features and progenies of PCL and PWM progenitors are not well known. For instance, despite evidence that the PWM is the main source of cerebellar interneurons (Leto et al., 2009; Silbereis et al., 2009; Fleming et al., 2013), a direct proof excluding other sources including the PCL is still missing.

Moreover, it is still unclear whether a lineage relationship exists between interneurons and astrocytes, as suggested by previous studies (Leto et al., 2012). Mice lacking the transcription factor Achaete-scute homolog-1 show increased astrocyte production at the expense of interneurons, suggesting that these lineages might originate from the same progenitor (Grimaldi et al.,

Received Dec. 23, 2014; revised March 22, 2015; accepted March 28, 2015.

Author contributions: E.P., K.L., A.B., and F.R. designed research; E.P., K.L., and C.R. performed research; C.R., M.F.-O., and L.L.-M. contributed unpublished reagents/analytic tools; E.P., K.L., C.R., and A.B. analyzed data; E.P., K.L., and A.B. wrote the paper.

This work was supported by the Ministry of Universities and Research [Research Programs of Relevant National Interest 2009 Program TBCZJB (F.R.) and Research Fund for the Promotion of Basic Research Grant RBFR10A01S (K.L.)] and the University of Turin. This study was also partly funded by the research grant BFU2013-48807-R from the Spanish Ministry of Economy and Competitivenes to Laura López-Mascaraque. We thank Mikio Hoshino, Silvia De Marchis, and Annarita DeLuca for critical reading of this manuscript and helpful suggestions. We are also indebted to Alexandra Lepiez and Magdalena Götz for kindly providing the LCMV plasmids, Verdon Taylor for the gift of the Confetti mutant line, Annarita DeLuca for technical help, and Daniele Imperiale for cyclin stainings. We dedicate this work in memory of Prof. F. Rossi for his continuous support and encouragement.

†Deceased on January 24, 2014.

The authors declare no competing financial interests.

Correspondence should be addressed to Annalisa Buffo, Department of Neuroscience Rita Levi-Montalcini, University of Turin, Neuroscience Institute Cavalieri Ottolenghi, Regione Gonzole 10, I-10043 Orbassano, Turin, Italy. E-mail: annalisa.buffo@unito.it.

C. Rolando's present address: Department of Biomedicine, University of Basel, CH-4058 Basel, Switzerland.

DOI:10.1523/JNEUROSCI.5255-14.2015

 0270-6474/15/357388-15$15.00/0

2009; Sudarov et al., 2011). Consistent with this view, a common origin of cerebellar interneurons and astrocytes has been suggested by previous fate-mapping studies (Mori et al., 2006; Silbereis et al., 2009; Sudarov et al., 2011; Fleming et al., 2013). However, it remained unsolved whether cerebellar interneurons and astrocytes derive from a single population of multipotent progenitors or from distinct pools of fate-restricted precursors. More recently, it has been proposed that a population of NSC-like progenitors generate both intermediate astrocyte precursors and transient amplifying progenitors for interneurons (Fleming et al., 2013). Nonetheless, the existence of such multipotent progenitors still awaits a full demonstration *in vivo*.

Here we addressed the phenotype and location of cerebellar progenitors producing interneurons. Our data show that postnatal astroglial-like PCL and PWM precursors possess different proliferative dynamics, exclude a contribution of the PCL to postnatal cerebellar neurogenesis, and demonstrate that astroglial-like progenitors of interneurons reside exclusively in the PWM. Finally, *in vitro* and *in vivo* clonal analyses indicate that these progenitors are bipotent and produce both interneurons and WM astrocytes.

Materials and Methods

Animals and surgical procedures. Experiments were performed on different mouse lines, including C57BL/6, GLAST::CreER^{T2} (Mori et al., 2006) crossed with R26R$^{LacZ/LacZ}$ (R26R^{LacZ}; Soriano, 1999) or R26R$^{EYFP/EYFP}$ (R26R^{YFP}; Srinivas et al., 2001), R26R$^{Confetti/+}$ (R26R^{Confetti}; Snippert et al., 2010), Pax2–green fluorescent protein (GFP; Pfeffer et al., 2002), β-actin–GFP (Okabe et al., 1997), and Ccnd2 (cD2 KO; Sicinski et al., 1996) of either sex. Day of vaginal plug detection was defined as embryonic day 0 (E0), and the day of birth was considered as postnatal day 0 (P0). All the surgical procedures were performed under deep anesthesia. Pups up to P5 were anesthetized by hypothermia, and pregnant mice were anesthetized by inhalation of isoflurane administered in conjunction with a mixture of 30% O_2/70% N_2O. After *in utero* electroporations, an analgesic (Rimadyl) was administered to pregnant mice to reduce postsurgical pain. All procedures were in accordance with the European Communities Council Directive European Communities Council (2010/63/EU), the National Institutes of Health guidelines, and the Italian Law for Care and Use of Experimental Animals (DL26/14) and were approved by the Italian Ministry of Health and the Bioethical Committee of the University of Turin.

Systemic and local administration of tamoxifen. To induce Cre recombination in GLAST::CreER^{T2}×R26R^{YFP} or R26R^{LacZ} mice, we administered tamoxifen (Tx; 20 mg/ml solution dissolved in corn oil) via subcutaneous injection for pups (600 μg/pup) or via oral gavage for pregnant mice (5 mg/40 g body weight). Clonal analyses in R26R^{Confetti} mice were performed by administering low Tx doses (1.2 μg/pup). To allow Cre recombination exclusively in PCL BG progenitors, we topically administered Tx citrate (Sigma-Aldrich) as described previously (Bi et al., 2011) with some modifications. We opened the skin and made a small incision on the skull that left intact the pial surface. We then placed Tx crystals on the pial surface. Finally, we carefully wiped the wound and closed it.

Thymidine analogs. Bromodeoxyuridine (BrdU; Sigma-Aldrich) and 5-ethynyl-2′-deoxyuridine (EdU; Invitrogen) were dissolved at 10 mg/ml in sterile saline and administered via intraperitoneal injection. The same dose of 100 μg/kg body weight was used for both analogs. EdU was injected 30 min before the animals were killed. For BrdU labeling, samples were incubated in 2N HCl for 20 min at 37°C, washed with borate buffer, pH 8.5, for 10 min, and processed for anti-BrdU antibody staining. EdU was detected using a commercial kit (Life Technologies) after the immunohistochemical reactions.

Lymphocytic choriomeningitis virus injection into the fourth ventricle and in the postnatal cerebellum. To permanently infect cells with an astroglial phenotype, we used an HIV-based lentiviral eGFP vector pseudotyped with the lymphocytic choriomeningitis virus (LCMV) glycoprotein generated according to the study by Buffo et al. (2008). After a deep anesthesia, P1–P5 pups were placed in a stereotaxic apparatus, and 0.3–0.5 μl of viral particle suspension (2.9×10^7 TU/ml) was injected in the cerebellar parenchyma with a picopump (WPI). Mice were then allowed to recover and killed after a defined time.

For *in utero* transduction, pregnant mice at 15 d of gestation were anesthetized deeply, and the uterine horns were exposed out of the abdominal wall moistened constantly with sterile PBS. Then, embryos were transilluminated by a cold light source to identify both the fourth ventricle and the cerebellum. One microliter of virus suspension mixed with fast green (2.5 mg/ml; Sigma-Aldrich) was injected in the ventricle cavity with a picopump. At the end of the procedure, the uterus was returned into the abdomen, the wound was sutured, and the pregnant mice recovered under a heating lamp. Injected embryos were allowed to develop normally and were analyzed at selected adult ages.

Histological and immunohistochemical procedures. Under anesthesia, animals were perfused transcardially with an appropriate volume of 4% paraformaldehyde (PFA) in 0.12 M phosphate buffer (PB), pH 7.2–7.4. Brains were removed, stored overnight in the same fixative at 4°C, washed in PBS, and finally cryoprotected in 30% sucrose in 0.12 M PB. The cerebella were then embedded and frozen over dry ice in OCT (Tissue-Tek), sectioned in the parasagittal plane at 30 μm using a cryostat, and collected in PBS (juvenile cerebella) or placed directly onto glass slides (P1–P15 cerebella). For immunolabeling, sections were incubated overnight at room temperature with the appropriated primary antibodies dissolved in PBS with 1.5% donkey or goat serum (Jackson ImmunoResearch) and 0.25% Triton X-100 (Sigma-Aldrich): anti-parvalbumin (PV; 1:1500, mouse monoclonal; Swant), anti-neurogranin (NG; 1:500, rabbit polyclonal; Millipore Bioscience Research Reagents); anti-Pax2 (1:200, rabbit polyclonal; Zymed), anti-NG2 (1:200; rabbit polyclonal; Millipore Bioscience Research Reagents), anti-β-galactosidase (β-gal; 1:20,000; rabbit polyclonal: Cappel); anti-S100β (1:1000, mouse monoclonal; Sigma), anti-Olig2 (1:500; rabbit polyclonal; Millipore Bioscience Research Reagents), anti-GFP (1:700, rabbit polyclonal; Invitrogen), anti-GFP (1:700, chicken polyclonal; Aves Labs), anti-BrdU (1:500, rat monoclonal; Abcam), anti-glial fibrillary acidic protein (GFAP; 1:1000, rabbit polyclonal; Dako), anti-βIII-tubulin (Tuj1; 1:200; mouse monoclonal; Sigma), anti-brain lipid binding protein (BLBP; 1:500; rabbit polyclonal; Abcam), anti-Ki67 (1:500; rabbit polyclonal; Novacastra); and anti-Sox9 (1:2000; rabbit polyclonal; generous gift from M. Wegner, University of Erlangen-Nüremberg, Erlangen, Germany). Sections were then exposed for 2 h at room temperature to secondary species-specific antibodies conjugated with Alexa Fluor 488, Alexa Fluor 555, or Alexa Fluor 647 (1:500; Invitrogen) or Cy3 (1:500; Jackson ImmunoResearch). Cell nuclei were visualized using 4′,6-diamidino-2-phenylindole (DAPI; Fluka). After processing, sections were mounted on microscope slides with Tris–glycerol supplemented with 10% Mowiol (Calbiochem).

For detection of β-gal, the high-sensitivity tyramide amplification kit (PerkinElmer Life and Analytical Sciences) was used (Buffo et al., 2008). For R26R^{Confetti} stainings, 50 μm serial sections obtained with a vibrating microtome (Leica) were incubated for 48 h at 4°C in primary antibody solution containing 1.5% donkey serum and 2% Triton X-100. Secondary antibody incubation was performed overnight in PBS with 1.5% donkey serum and 0.5% Triton X-100.

For immunohistochemical labeling of cyclins, fixed cerebella were embedded in paraffin wax and cut in 5 μm sections, which were treated with 3% H_2O_2 for 10 min and incubated overnight at 4°C with anti-cyclin D1 (cD1; 1:500; LabVision; or 1:100; Abcam) or anti-cD2 (1:500; LabVision) antibodies. The sections were incubated with secondary antibodies, followed by the Vectastain Elite kit (Vector Laboratories) for 30 min each, and finally revealed by reaction with 3,3′-diaminobenzidine. The sections were dehydrated and coverslipped.

Cell cultures of cerebellar progenitors. Postnatal cultures were performed by dissecting the PWM of cerebellar parasagittal slices obtained by means of a tissue chopper (McIlwain). Tissues were incubated 5 min at 37°C in 0.05% trypsin EDTA (Gibco), and then the trypsin inhibitor (Gibco) was added. Samples were triturated and centrifuged to obtain a cell suspension. For clonal analyses, cells were plated on 12 mm glass coverslips coated with poly-D-lysine at a density of 1000 cells/coverslip.

Cells were maintained in Neurobasal medium supplemented with 1× B27 and N2, 2 mM glutamine, 100 U/ml penicillin/streptomycin (Gibco), 0.6% glucose (Sigma-Aldrich), 20 ng/ml epidermal growth factor (Miltenyi Biotech), and 10 ng/ml basic fibroblast growth factor (Miltenyi Biotech; Qian et al., 2000; Milosevic and Goldman, 2004). Clonal development was monitored by daily microscope inspection. In clonal cocultures, wild-type and β-actin–GFP-expressing cells were mixed in a 1:1 ratio.

Ex vivo *electroporations and organotypic slice cultures.* Clonal analysis was performed by a modification of the *StarTrack* approach (García-Marqués and López-Mascaraque, 2013) by using a ubiquitous promoter [UbiquitinC (UbC)]. Briefly, *StarTrack* is based on the genomic incorporation of 12 plasmids in which expression of six different fluorescent proteins, localized in either the cytoplasm or the nucleus, is now driven by the UbC promoter to replace the original GFAP one. Each construct incorporates inverted terminal repeat sequences recognized by the *piggyBac* transposase introduced in another plasmid to allow the genomic integration of these constructs. This results in a unique color combination code identifying both neuronal and glial clones derived from single progenitors. Coelectroporations of these 13 constructs were performed *ex vivo* on P0–P2 cerebella. Briefly, brains were dissected out and maintained in sterile ice-cold PBS supplemented with 0.6% of glucose. After careful removal of the meninges, 0.5 μl of plasmid mixed with fast green (2–5 mg/ml) was injected with a glass capillary into the cerebellar parenchyma. To enhance nuclear membrane permeability, we added 0.5 μl of trans-cyclohexane-1,2-diol (100 mg/ml; Sigma-Aldrich) to the plasmid solution, as indicated by De la Rossa et al. (2013). Two minutes after plasmid mixture injection, we delivered one train of 10 square pulses (50 V, 50 ms at 950 ms intervals), using a BTX electroporator (Holliston). After electroporation, the cerebellum was isolated and sliced parasagittally at 300 μm using a tissue chopper. Slices were collected in ice-cold PBS with 0.6% of glucose. *Ex vivo* electroporated slices labeled by fast green were selected and placed rapidly on a Millicell culture insert (BD Biosciences). Organotypic slices were maintained at 37°C in 5% CO_2 in Eagle medium (Invitrogen) supplemented with 2 mM glutamine, 32 mM glucose, 20 U/ml penicillin/streptomycin, 10 mg/ml bovine serum albumin (Sigma), and 1× B27 supplement (Gibco) as described previously (De Luca et al., 2015). Seven days later, slices were fixed for 30 min in 4% PFA and processed as described above.

Image processing, clone evaluation, and data analysis. Histological specimens were examined using an E-800 Nikon microscope connected to a color CCD camera and a Leica TCS SP5 confocal microscope. Adobe Photoshop 6.0 (Adobe Systems) was used to adjust image contrast and assemble the final plates. Quantifications were performed on confocal images by NIH ImageJ software (http://rsb.info.nih.gov/ij/), as described previously (Leto et al., 2011). In some instances, we applied the colocalization analysis provided by the LAS AF software (Leica) to display in white marker coexpression at the pixel level.

Measurements were derived from at least three sections per animal. Two to five animals were analyzed for each time point or experimental condition. For *in vitro* experiments, data were derived from three coverslips of three different experiments. Evaluations of the modified ubiquitous *StarTrack* construct expression and $R26R^{Confetti}$ mice were performed by confocal analysis using acquisition parameters described previously (Snippert et al., 2010; García-Marqués and López-Mascaraque, 2013).

Analyses of GLAST::$CreER^{T2}$ and LCMV experiments included only VZ derivatives and did not consider occasional granule cells found up to perinatal ages, because these derive from the distinct germinal site of the RL/EGL.

In vitro single clones were identified as composed by (1) juxtaposed elements derived by an isolated cell (as confirmed by microscope inspection after plating) and (2) nearby cells if placed within 20 μm from the clone core.

Cells with the same fluorescent marks, as detected by confocal inspection, were considered as clones in *StarTrack*-labeled organotypic cultures. For *in vivo* clonal analysis of $R26R^{Confetti}$ mice, the whole cerebellum was analyzed using a fluorescence microscope to identify red fluorescent protein (RFP)-, yellow fluorescent protein (YFP)-, and GFP-expressing cells. Labeled cells were mapped and classified using morphological criteria for astrocytes and interneurons. Cells identity was confirmed by PV or GFAP immunohistochemistry. Clones were defined according to (1) expression of the same fluorescent color code and (2) lobular localization. Because Tx was administered at P3, when lobular organization is already established (Sudarov and Joyner, 2007), we considered that PWM progenitors would likely produce cells only within the very same lobule when already placed intralobularly, or in adjacent lobules, in the case of progenitors positioned in the PWM at the basis of two contiguous lobules. Thus, we defined a clone composed of cells within the same lobule. However, we interpreted color-matched interneurons in adjacent lobules as part of the same clone with astrocytes found in the WM shared by the adjacent lobuli.

Statistical significance was assessed by GraphPad Prism software (GraphPad Software) by applying unpaired Student's *t* test or one-way ANOVA with Bonferroni's multiple comparisons test; $p < 0.05$ was considered to be statistically significant. Data are expressed as averages ± SEMs.

Results

PCL and PWM progenitors are different in their proliferative activities

To highlight similarities or differences in PCL and PWM progenitors, we examined the expression of cyclins and cell proliferation at these germinal sites. Cyclins are regulators of the cell cycle G_1/S-phase transition through the activation of cyclin-dependent kinases (Sherr, 1995; Sherr and Roberts, 1999) and comprise isoforms that are expressed differentially in progenitors with distinct proliferative and differentiation potentials (Glickstein et al., 2007). In the cerebellum of wild-type mice at P4, cD2-positive ($cD2^+$) cells were located mostly in the PWM (Fig. 1*A*), whereas $cD1^+$ nuclei were for the vast majority confined along a thin row below the Purkinje cell perikarya (Fig. 1*B*). Here, the 95.7 ± 0.8% of $cD1^+$ nuclei displayed astroglial/NSC traits, as detected by positivity for BLBP (Anthony et al., 2004, 2005; Fig. 1*C*). The same pattern of cD1 expression was retained in age-matched cD2 KO mice (Fig. 1*D*).

Cell proliferation analysis in wild-type and cD2 KO mice revealed that $BrdU^+$ cells decrease strongly in the PWM of mutant mice, but no changes occur in actively proliferating cells within the PCL region (Fig. 1*E*). Similar results were obtained by the analysis of the S-phase index (namely $BrdU^+$ nuclei/total number of DAPI-stained nuclei; Fig. 1*F*), showing that cD2 does not participate in the regulation of the cell cycle dynamics of PCL progenitor cells, whereas it supports cell division in the PWM.

We further focused on the proliferation of PCL and PWM progenitors with astroglial/NSC traits that were tagged in GLAST::$CreER^{T2}$×$R26R^{YFP}$ mice (Mori et al., 2006). In this line, the inducible form of Cre is expressed in the locus of the astrocyte-specific glutamate/aspartate transporter (GLAST), thereby targeting progenitors producing cerebellar neurons and glia during recombination at early embryonic stages (E12, E14; Mori et al., 2006). Postnatal (P3) Tx administration induced reporter gene expression in bona fide astroglial-like progenitors clustered in both the PCL and PWM (see below; Fig. 1*J*), as well as in early postmitotic astrocytes. To examine the proliferation rate of both astroglial-like progenitors and their early progeny, we performed a BrdU pulse-chase experiment, followed by EdU injection before the animals were killed. In this way, a first DNA duplication phase (first S-phase) was marked attributable to the incorporation of BrdU, whereas a possible reentry in the cell cycle of the formerly BrdU-labeled progenitors could be tagged by the integration of EdU in the DNA duplicated during the second

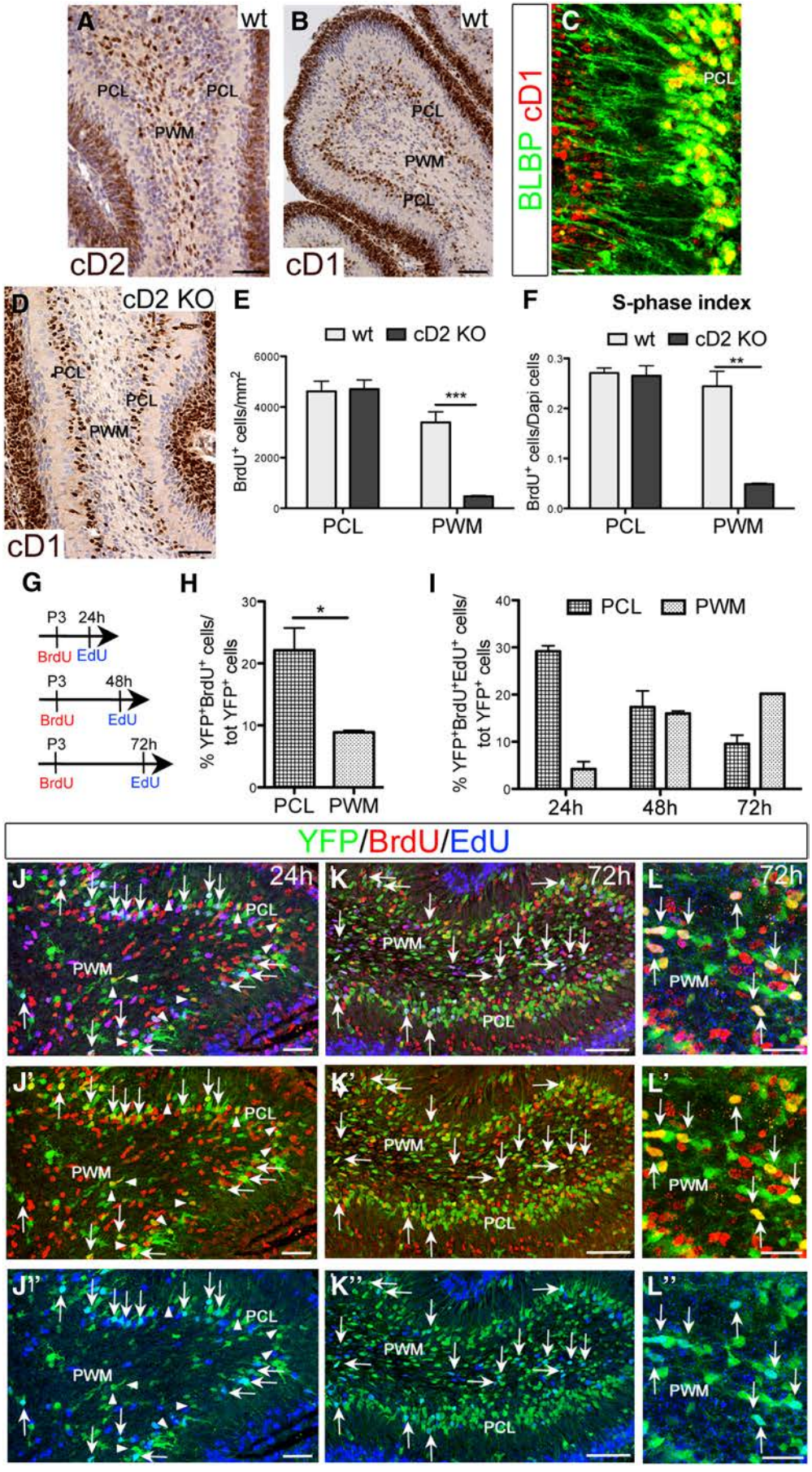
A
wt
PCL
PCL
PWM
cD2
B
wt
PCL
PWM
PCL
cD1
BLBP cD1
C
PCL
D
cD2 KO
PCL
PCL
PWM
cD1
E
wt
cD2 KO
6000
4000
2000
0
BrdU+ cells/mm2
***
PCL
PWM
F
S-phase index
wt
cD2 KO
0.3
0.2
0.1
0.0
BrdU+ cells/Dapi cells
**
PCL
PWM
G
P3 24h
BrdU EdU
P3 48h
BrdU EdU
P3 72h
BrdU EdU
H
30
20
10
0
% YFP+BrdU+ cells/ tot YFP+ cells
*
PCL PWM
I
40
30
20
10
0
% YFP+BrdU+EdU+ cells/ tot YFP+ cells
PCL
PWM
24h
48h
72h
YFP/BrdU/EdU
J
24h
PCL
PWM
K
72h
PWM
PCL
L
72h
PWM
J'
PCL
PWM
K'
PWM
PCL
L'
PWM
J''
PCL
PWM
K''
PWM
PCL
L''
PWM

S-phase (see experimental scheme in Fig. 1*G*). At 24 h, cell proliferation, as revealed by BrdU labeling in YFP$^+$ cells, was threefold higher in the PCL compared with the PWM (BrdU$^+$YFP$^+$ cells among total YFP$^+$ cells: 22.10 ± 3.6% in the PCL and 8.9 ± 0.3% in the PWM, unpaired *t* test, $p = 0.036$; Fig. 1*H* and arrowheads in *J*,*J*′). Additionally, a large fraction of PCL progenitors reentered the cell cycle at 24 h, whereas a significant fraction of PWM progenitors started a second S-phase only after 48 h (PCL: one-way ANOVA, $F_{(2,4)} = 8.555$, $p = 0.03$, $n = 2$–3, main effect of time; PWM: one-way ANOVA, $F_{(2,4)} = 6.957$, $p = 0.04$, $n = 2$–3, main effect of time; Fig. 1*I*–*L*). Collectively, these data suggest a faster proliferation in the PCL and show distinct proliferative activities in PCL and PWM.

Cerebellar interneurons and glial cells derive from GLAST$^+$ progenitors

As a next step, we addressed the fate of cerebellar GLAST$^+$ cells at late embryonic (E17; Fig. 2*A*–*E*) and postnatal (Fig. 2, P1 in *F*–*H* and P6 in *I*–*K*) stages by following the GLAST::CreER^{T2}-mediated recombination of the *Rosa26–YFP* or *Rosa26–LacZ* alleles (hereafter referred to as YFP or β-gal, respectively) after Tx administration. Phenotypes of reporter-expressing cells were analyzed at P30 and identified by double immunohistochemistry with cell type-specific markers (Fig. 2*A*–*D*,*F*,*G*,*I*,*J*).

When Tx was administered at E17, β-gal$^+$ cells included all the different classes of GABAergic interneurons of the cortex: PV$^+$ interneurons in the molecular layer (ML; Fig. 2*A*; Bastianelli, 2003), NG$^+$ Golgi cells (Fig. 2*B*; Simat et al., 2007), and Lugaro cells in the granular layer (GL; Fig. 2*C*) and deep nuclei interneurons. In addition, S100β$^+$ BGs and astrocytes were also labeled throughout the cerebellar parenchyma (Fig. 2*D*,*E*). Similarly, P1 induction resulted in β-gal$^+$ inhibitory interneurons mostly located in the ML (Fig. 2*F*,*H*), BGs, and parenchymal astrocytes (Fig. 2*G*,*H*). Interestingly, when Tx was administered at P6, β-gal$^+$ interneurons were infrequent and correspond exclusively to PV$^+$ stellate cells (Fig. 2*I*–*I*″,*K*), whereas the majority of β-gal$^+$ cells were astrocytes (Fig. 2*J*,*K*). Up to perinatal ages, a small proportion of β-gal$^+$ cells were immunopositive for the marker Olig2 (Fig. 2*E*,*H*,*K*) and exhibited typical morphological features of cerebellar oligodendrocytes (OLs; data not shown). Thus, within GLAST-expressing cells, proliferative progenitors produce distinct types of GABAergic interneurons and glial cells at perinatal ages, whereas their neurogenic activity declines with time.

To better understand the differentiation potential of GLAST$^+$ progenitors and interneurogenesis, we focused on postnatal ages and analyzed reporter-expressing cells shortly after Tx administration. Tx was administered at P3, a time point of intense interneuron production (Fig. 3*A*). After a 1 d chase period, the majority of YFP$^+$ cells expressed the astroglial marker Sox9 and localized in the PCL and PWM (Fig. 3*B*,*E*,*F*,*F*′), confirming that recombined cells initially display astroglial traits. Conversely, YFP$^+$ cells expressing the immature interneuronal marker Pax2$^+$ were very rare and localized in the PWM (Fig. 3*B*,*G*,*H*,*H*′). Moreover, between 1 and 7 d after Tx, the fraction of YFP$^+$Pax2$^+$ cells in the PWM increased over time, implying a progressive acquisition of the interneuron fate (Fig. 3*C*). Conversely, high percentages of YFP$^+$ cells in the PWM colocalized with the astrocytic marker Sox9 at all time points without significant variations (Fig. 3*C*). To strengthen evidence for cell neogeneration, we pulsed mice with BrdU immediately after Tx administration (Fig. 3*A*). At all examined stages, we found a fraction of YFP$^+$ cells double labeled for both Pax2 and BrdU, or Sox9 and BrdU (Fig. 3*E*–*M*″, arrowheads). Importantly, Pax2$^+$BrdU$^+$YFP$^+$ cells were enriched in the PWM compared with the cerebellar cortex (data not shown) and peaked at 3 d chase (Fig. 3*D*). Subsequently, YFP$^+$ newly generated interneurons progressively left the PWM, moved to the cortical districts, and settled in the ML (Fig. 3*D*,*M*–*M*″). In summary, BrdU labeling and GLAST::CreER^{T2} lineage tracing indicate that proliferative astroglial-like precursors generate both Sox9$^+$ astrocytes and Pax2$^+$ GABAergic interneurons up to the first postnatal week of cerebellar development.

Progenitors in the PCL do not generate GABAergic interneurons

Short-term fate-mapping analysis (see above) and previous BrdU-based birthdating and lineage studies (Leto et al., 2009; Silbereis et al., 2009; Fleming et al., 2013) provide evidence that the PWM is the main source of cerebellar interneurons. However, direct evidence of the exclusive localization of primary progenitors originating interneurons in the PWM is still missing. The PCL might also host such precursors.

To examine whether GLAST$^+$ PCL progenitors produce interneurons, we developed a method to selectively label PCL astroglial precursors excluding those in the PWM. We reasoned that PCL progenitors exclusively possess end feet contacting the pial surface being derived by delaminating RGs that maintained the basal process (Yamada and Watanabe, 2002). Thus, we applied small quantities of Tx on the surface of postnatal (P3) GLAST::CreER^{T2}×R26R^{YFP} cerebella and analyzed the fate of reporter-expressing cells 20 d later (Fig. 4*A*). Shortly after Tx administration, virtually all YFP$^+$ cells were in the PCL (79 ± 3.3% of total YFP$^+$ cells; Fig. 4*B*,*B*′), and many were labeled by the proliferative marker Ki67 (Fig. 4*C*, arrow and arrowheads). The remaining tagged cells were found in the GL (16 ± 3.1% of YFP$^+$ cells) or rarely in the PWM (3.6 ± 1.1% of YFP$^+$ cells; Fig. 4*B*). After 20 d, the vast majority of YFP$^+$ cells were mature GFAP$^+$ BG cells (73 ± 2.6% of YFP$^+$ cells; Fig. 4*D*,*E*,*E*′), whereas only few astrocytes were found in the GL (20.3 ± 2.8% of YFP$^+$ cells) or in the WM (6.7 ± 0.2% of YFP$^+$ cells). Importantly, we never observed YFP$^+$ interneurons derived from PCL precursors (Fig. 4*F*). On the whole, these experiments demonstrate that, in physiological conditions, PCL progenitors are not able to generate interneurons.

←

Figure 1. Postnatal progenitors in PCL and PWM niches express diverse cyclins and possess different proliferative dynamics. Different D-type cyclins are expressed preferentially in PCL and PWM of P4 mice (***A–D).*** In wild-type animals, cD2$^+$ cells are mostly located in the PWM (***A***), whereas cD1$^+$ nuclei are primarily segregated along the PCL (***B***). Here, cD1 is expressed in the vast majority of cells expressing the astroglial/NSC marker BLBP (***C***). ***D***, Age-matched cD2 KO mice maintain the same pattern of cD1 distribution. ***E***, Histograms indicate that dividing cells, tagged by BrdU 2 h before the animals were killed, are significantly decreased in the PWM of cD2 KO mice (unpaired *t* test, $p = 0.0010$, $n = 3$–4), whereas no changes are detected in the PCL region. ***F***, Analysis of the S-phase index provides similar results (unpaired *t* test, $p = 0.0025$, $n = 3$–4). ***G***, Experimental scheme. Tx is administered at P3, to tag PCL and PWM GLAST$^+$ cells and their derivatives. A pulse of BrdU at P3 is followed by a pulse of EdU 30 min before the animals are killed. ***H–L***, Proliferative dynamics of PCL and PWM progenitors are examined in GLAST::CreER^{T2}×R26R^{YFP} mice through the double-analog technique. Active proliferating tagged cells (YFP$^+$BrdU$^+$, arrowheads in ***J–J′***) are more abundant in the PCL compared with the PWM. YFP$^+$ cells incorporating both thymidine analogs (arrows in ***J–L***) are located preferentially in the PCL at 24 h intervals from the first S-phase (***I***, arrows in ***J-J′***) or in the PWM at longer intervals (***I***, arrows in ***K–L″***). Errors bars indicate SEM. Scale bars: ***C***, 20 μm; ***A***, ***B***, ***D***, 40 μm; ***J–J″***, ***L-L″***, 50 μm; ***K–K″***, 100 μm .

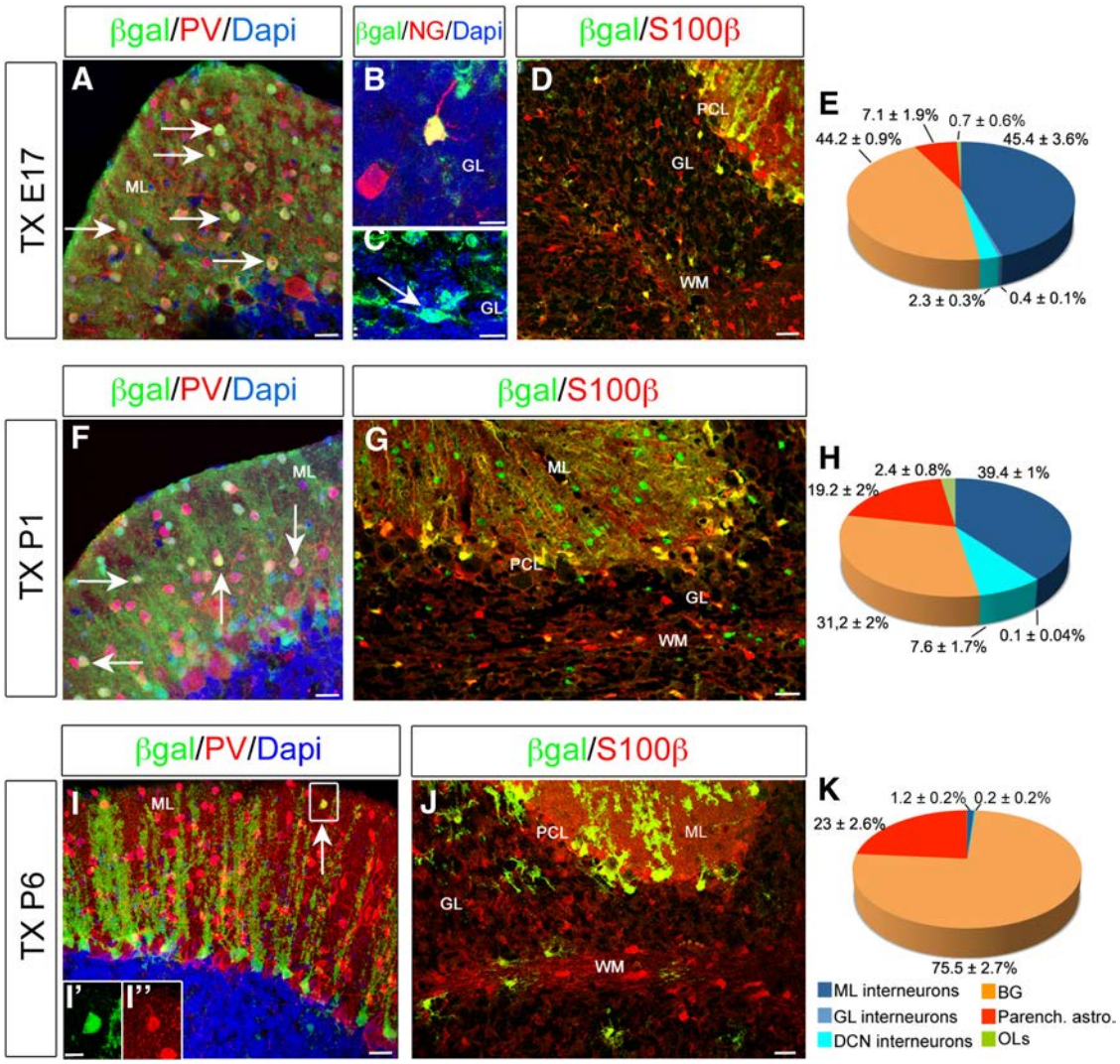

Figure 2. Fate mapping of GLAST$^+$ progenitors. Characterization of reporter-tagged cells at P30 after recombination at E17 (***A–E***), P1 (***F–H***), or P6 (***I–K***) in GLAST::CreER^{T2}×R26R^{lacZ} mice. When Tx is administered at E17, β-gal$^+$ cells generate all the different classes of inhibitory interneurons of the cortex and deep nuclei (***E***): PV$^+$ basket and stellate cells of the ML (***A***), NG$^+$ Golgi cells (***B***), and Lugaro cells of the GL (arrows in ***C***). In addition, both S100β$^+$ BG cells in the PCL and parenchymal astrocytes are produced (***D***, ***E***). β-gal$^+$ cells tagged at P1 still produce GABAergic interneurons (***F***, ***H***), parenchymal astrocytes, and BG cells (***G***, ***H***). At later postnatal stages, β-gal$^+$ cells rarely differentiate in ML interneurons (arrow in ***I*** and insets ***I′***, ***I″***), whereas astroglial phenotypes prevail (***J***, ***K***). Data are expressed as averages ± SEMs. $n = 2$–3. Scale bars: ***B***, ***C***, ***I′***, ***I″***, 10 μm; ***A***, ***F***, ***I***, 20 μm; ***D***, ***J***, 30 μm; ***G***, 40 μm.

Astroglial-like neurogenic progenitors localize in the postnatal PWM

Based on the above results, we exclude that the PCL is a neurogenic niche and predict that PWM exclusively hosts primary progenitors generating interneurons in the postnatal cerebellum. To test this hypothesis, we performed a viral-based fate mapping. We targeted the PWM at P3/P5 (Fig. 5*A*) with an LCMV-pseudotyped lentiviral vector encoding for an enhanced GFP that displays a particular tropism for astroglial cells (Stein et al., 2005; Buffo et al., 2008).

At 2 d post-infection (dpi), the majority of GFP$^+$ cells that remained in the PWM expressed the astrocytic markers BLBP and Sox9 (Fig. 5*B*, arrows in *C*,*D*). Interestingly, a fraction of PWM GFP$^+$ cells expressed also the proliferative marker Ki67 (Fig. 5*E*, arrows) and markers for neurogenic progenitors, such as Sox2 and Nestin (Pevny and Nicolis, 2010; Bonaguidi et al., 2011; data not shown). No interneurons were observed at 2 dpi (Fig. 5*B*,*F*). At 4 dpi, the majority of infected cells still expressed astroglial markers (Fig. 5*B*, arrows in *G*), but few Pax2$^+$GFP$^+$ cells appeared in the PWM (Fig. 5*B*, arrows in *H*). In line with an *ex novo* generation of interneurons from GFP$^+$ cells, 12 ± 4% of GFP$^+$ cells with a neuronal morphology showed BrdU incorporation 4 d after a single thymidine analog pulse at the moment of virus injection (Fig. 5*I*). Similarly, 12.7 ± 5.1% of astroglial cells at this time were positive for BrdU (Fig. 5*J*, arrows), revealing that at least part of the astrocytes were produced by tagged progenitors and not just directly infected. One week after LCMV infection, the total number of GFP$^+$ interneurons had significantly expanded within the whole GFP$^+$ population (Fig. 5*B*). Of note, at 7 dpi, the majority of tagged interneurons (69 ± 4% of total GFP$^+$ interneurons) had already reached the ML and positioned themselves just below the EGL, in which they continued to express Pax2 and displayed an immature morphology (Fig. 5*K*, arrow). Scattered interneurons also appeared in transit to exit the PWM (Fig. 5*L*, arrow) or had already approached the ML and acquired a more mature morphology (extended multipolar processes, Pax2 negativity; Fig. 5*M*, arrow). At this stage, ~20% among GFP$^+$ interneurons were still found in the PWM (Fig. 5*N*,

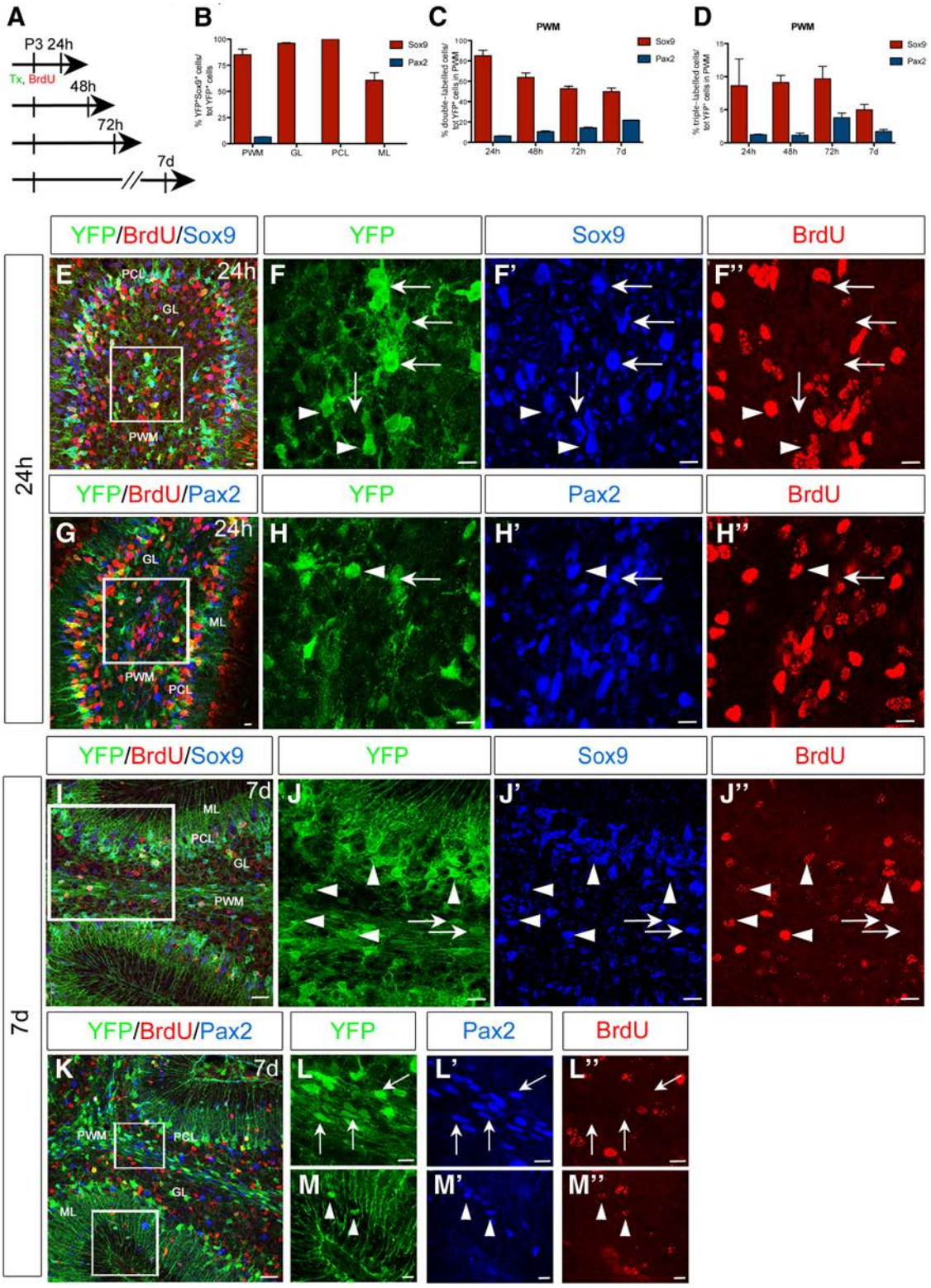

Figure 3. Short-term analysis of GLAST $^{+}$ progenitors. Analysis of recombined progenitors shortly after Tx injection at P3 (***A***). The majority of recombined cells expresses the astroglial marker Sox9 and is distributed in all the cortical layers and PWM (***B***, ***E***, arrows in ***F–F″***). Conversely, only in the PWM does a small fraction of YFP $^{+}$ cells colocalize with the interneuron marker Pax2 (***B***, ***G***, arrow in ***H–H″***). ***C***, In the PWM, YFP $^{+}$Pax2 $^{+}$ cells increase progressively from 48 h to 7 d after Tx treatment (***C***; one-way ANOVA, $F_{(2,4)} = 42$, $p = 0.02$, $n = 2–3$, main effect of time), whereas YFP $^{+}$Sox9 $^{+}$ astrocytes remain constant (one-way ANOVA, $F_{(2,4)} = 0.061$, $p = 0.9783$, $n = 2–3$, main effect of time). ***D***, Newly generated YFP $^{+}$ cells tagged by BrdU immediately after Tx administration are found at all time points (arrowheads in ***F–F″***, ***H–H″***, ***J–J″***, ***M–M″***). Seven days after Tx treatment, YFP $^{+}$ cells generate Sox9 $^{+}$ BG cells in the PCL and parenchymal astrocytes of the GL and WM (***I***, ***J***). In addition, a fraction of GLAST-derived Pax2 $^{+}$ interneurons has already reached their final cortical position (***K–M***). Boxes in ***E***, ***G***, ***I***, and ***K*** are magnified and shown as single-channel images. Scale bars: ***E–H″***, ***L***, ***M***, 10 μm; ***J–J″***, 15 μm; ***I***, ***K***, 30 μm.

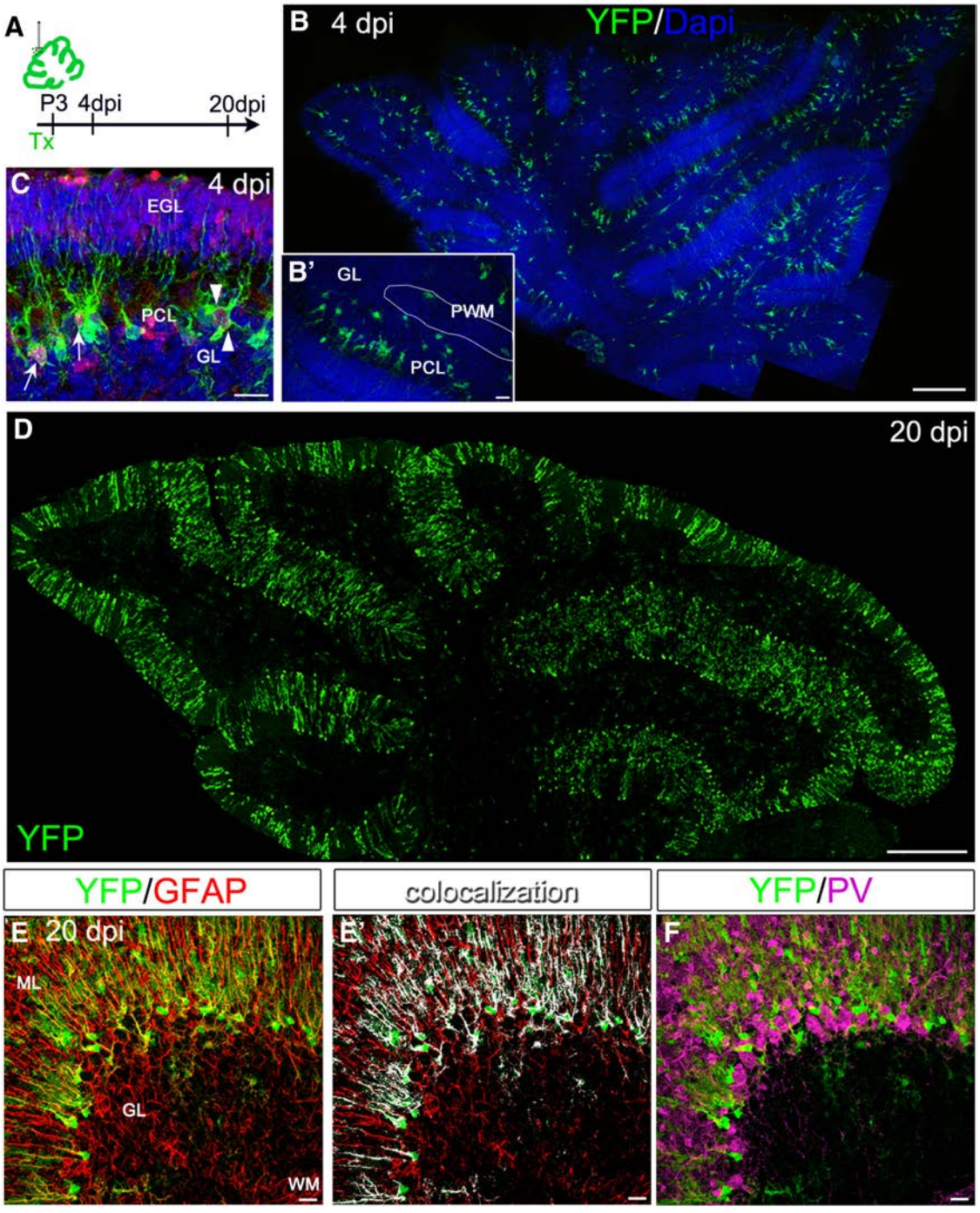

Figure 4. Selective labeling and fate mapping of PCL precursors. ***A***, Schematic representation of the experimental procedure. ***B***, ***B′***, The majority of YFP $^{+}$ cells analyzed 4 d after superficial Tx administration is located in the PCL and rarely found in the PWM. ***C***, YFP $^{+}$ cells in the PCL express the proliferative marker Ki67 (arrows). Duplets of dividing Ki67 $^{+}$YFP $^{+}$ cells are also found (arrowheads). ***D***, Whole section of a cerebellum superficially induced 20 d earlier showing almost exclusive recombination in BG within the PCL and lack of YFP $^{+}$ cells in the WM. The progeny of tagged cells consists of GFAP $^{+}$ BG and some astrocytes in the GL (***E***). Pixels decorated by positivity for both YFP and GFAP are represented in white in ***E′***. No YFP $^{+}$PV $^{+}$ interneurons are found (***F***). Scale bars: ***B′***, ***C***, ***E***, ***F***, 20 μm; ***B***, ***D***, 500 μm.

arrow). Starting from 7 dpi, PWM GFP $^{+}$ astrocytes expressed the mature markers GFAP (Fig. 5*O*, arrows) and S100β (data not shown). At later time points (15 dpi), the absolute number of both interneurons and astrocytes increased progressively, further demonstrating *ex novo* generation (total GFP $^{+}$ interneurons: 4 dpi, 11 $\pm$ 4 cells; 7 dpi, 18.25 $\pm$ 3.4 cells; 15 dpi, 92.3 $\pm$ 16 cells; one-way ANOVA, $F_{(3,10)} = 31.71$, $p < 0.0001$, $n = 3$–4, *post hoc* Bonferroni's test showed significant differences for 2, 4, and 7 dpi vs 15 dpi; total GFP $^{+}$ astrocytes: 2 dpi, 52.5 $\pm$ 10.2 cells; 4 dpi, 65 $\pm$ 8.19 cells; 7 dpi, 45.8 $\pm$ 4.9 cells; 15 dpi, 139.3 $\pm$ 33.7 cells; one-way ANOVA, $F_{(3,10)} = 6.851$, $p = 0.0087$, $n = 3$–4, *post hoc* Bonferroni's test showed significant differences for 2 and 7 dpi vs 15 dpi). Notably, virtually all GFP $^{+}$ astrocytes were found in the WM, showing that these cells did not migrate away from their site of generation and differentiated there as WM fibrous astrocytes. Thus, selective labeling of PWM postnatal astroglial progenitors confirms that this site hosts primary interneuron progenitors and specifically generates WM astrocytes.

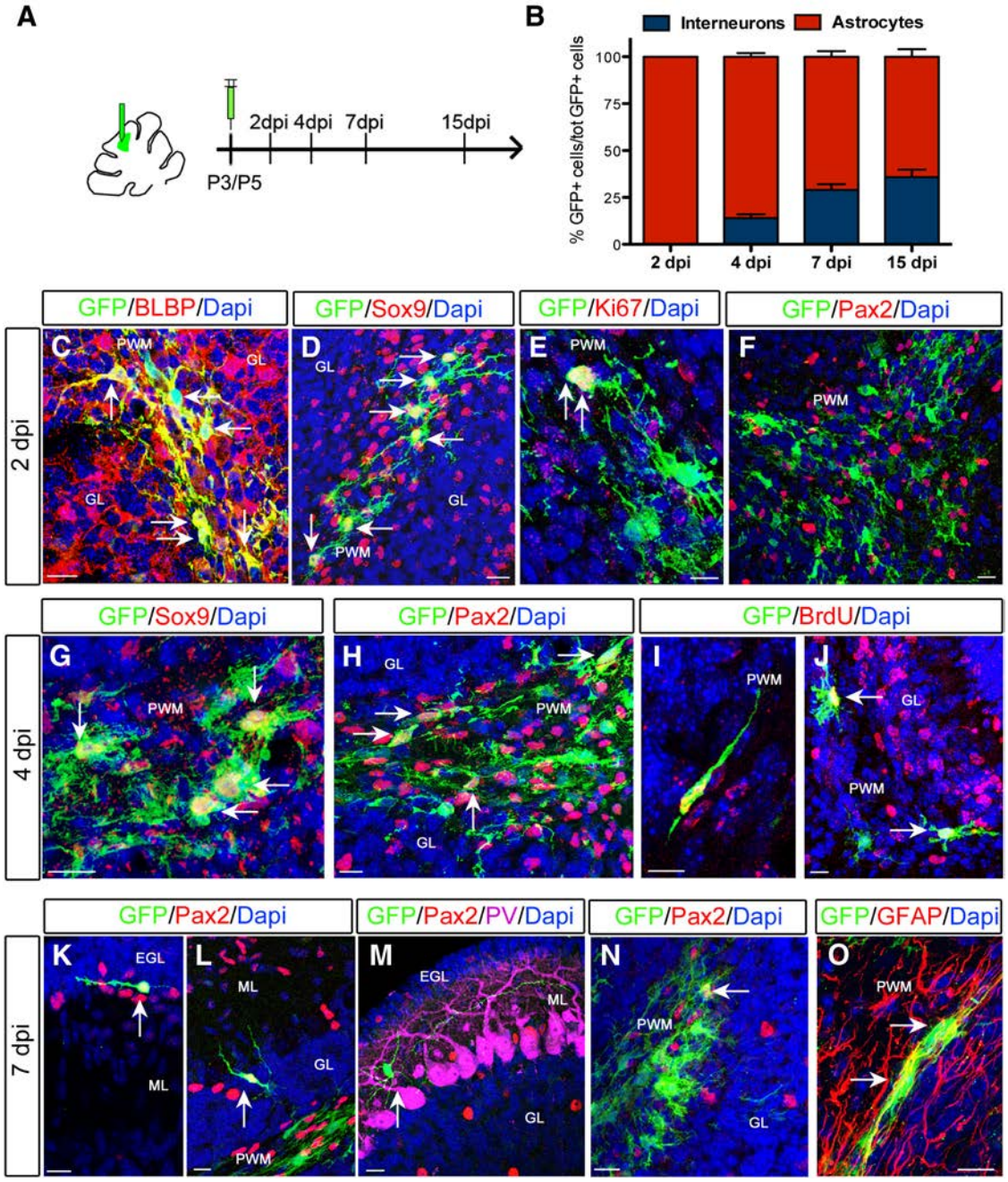

Figure 5. Phenotype and lineage of postnatally LCMV-infected cells. ***A***, Experimental procedure and timeline of the experiment. ***B***, Quantification of the percentage of Pax2 $^{+}$ interneurons or Sox9 $^{+}$ astrocytes in the GFP $^{+}$ population at different time points after lentiviral injection (astrocytes: one-way ANOVA, $F_{(3,10)} = 56.33$, $p < 0.0001$, $n = 3–4$, *post hoc* Bonferroni's test shows statistically significant differences for all the compared time points; interneurons: one-way ANOVA, $F_{(3,10)} = 56.33$, $p < 0.0001$, $n = 3–4$, *post hoc* Bonferroni's test shows statistically significant differences for all the compared time points). Shortly after LCMV injection, only astrocytes are infected, as demonstrated by the expression of BLBP (***C***) and Sox-9 (***D***) in GFP $^{+}$ cells (arrows). Labeled cells in the postnatal cerebellum mainly reside in the PWM (arrows in ***C–F***). Some of them proliferate actively (arrows in ***E***). No Pax2 $^{+}$ immature interneurons express the reporter protein (***F***). At 4 dpi, the majority of GFP $^{+}$ cells continue to display astroglial features (arrows in ***G***). However, some GFP $^{+}$ cells expressing Pax2 start to be observed (***H***, arrows). Newly generated cells with either a neuronal (***I***) or astroglial (***J***) morphology are positive for BrdU (arrows). One week after injection, Pax2 $^{+}$ interneurons derived from LCMV-infected cells are migrating through the cortex (***K–M***, arrows). The majority of them has already reached the ML and is located at the border of the EGL (***K***, arrows), whereas some are entering the ML from the GL (***L***, arrows). Interneurons positioned in the ML downregulate Pax2 expression and display a more branched morphology resembling that of mature interneurons (***M***, arrows). However, few interneurons are still located in the PWM (arrows in ***N***). Newly generated astrocytes reside in the WM and express mature markers, such as GFAP (***O***, arrows). Errors bars indicate SEM. Scale bars, 20 μm.

Neurogenic and gliogenic potential of PWM and VZ astroglial-like progenitors

PWM astroglial-like progenitors generate both interneurons and WM astrocytes. We next asked whether this lineage is maintained at other developmental stages. To this aim, we infected PWM cells at P1 and P5 with the LCMV and killed the mice at P30. In addition, we extended this analysis to an embryonic stage (E15) when we selectively transduced ventricular RG (Fig. 6*B*, arrow), from which PWM progenitors are postulated to delaminate during embryogenesis (Altman and Bayer, 1997; Mathis and Nicolas, 2003).

The differentiation potential of the infected progenitor cells varied during cerebellar development (Fig. 6*A*). Notably, the pro-

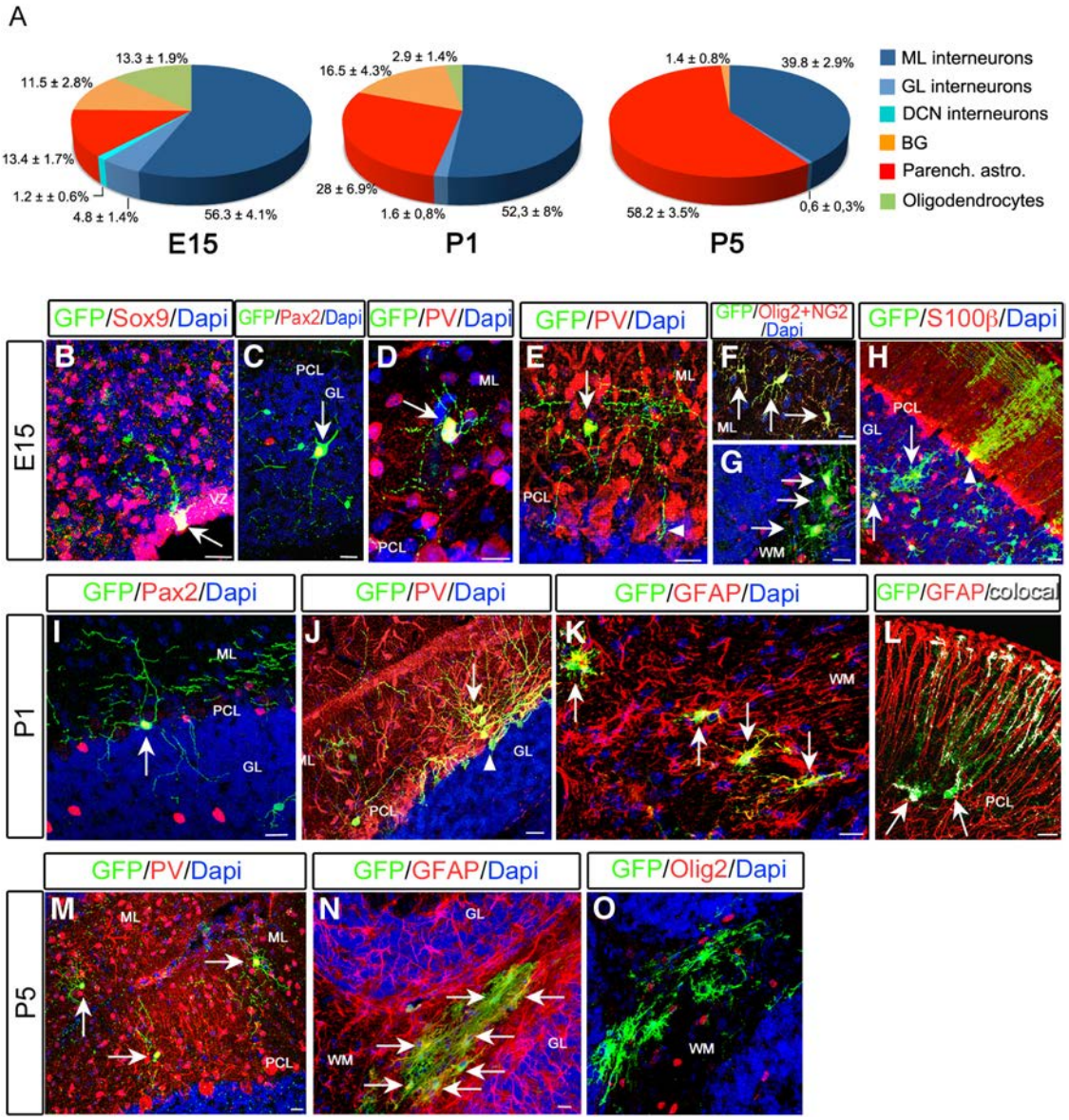

Figure 6. Fate analysis of LCMV-infected cells at different developmental stages. ***A***, Proportions (indicated as averages ± SEMs) of mature phenotypes generated at P30 by LCMV-infected progenitors at different stages during the embryonic (E15), early (P1), and later (P5) postnatal development. ***B***, LCMV injected in the fourth ventricle transduces RG cells lining the ventricular surface (arrow). Both interneurons (arrows and arrowhead in ***C–E***, ***I***, ***J***, ***M***) and glial cells (arrows in ***F–H***, ***K***, ***L***, ***N***) derive from LCMV-infected cells but to various extents during development. Different categories of interneurons are recognized by their morphology, location in the cerebellar cortex, and expression of typical markers (***C–E***, ***I***, ***J***, ***M***). ***C***, ***I***, Pax2$^+$ Golgi cells in the GL originate from early progenitors (E15, P1). ***D***, ***E***, ***J***, ***M***, Postnatally infected progenitors mainly generate interneurons of the most superficial layers (arrows). PV$^+$ basket cells settle close to Purkinje cell somata that they contact by means of specialized axonal terminals (i.e., the pinceau; see arrowheads in ***E***, ***J***). OLs in the ML (***F***, arrows) and the WM (***G***, arrows) are found exclusively after early infections, in addition to parenchymal astrocytes (***H***, arrows) and BG (***H***, arrowhead). Postnatal injections give rise to GFAP$^+$ astrocytes of the WM (arrows in ***K***, ***N***) and more rarely to BGs (***L***, arrows). Pixels decorated by positivity for both GFP and GFAP are represented in white in ***L***. ***O***, No Olig2$^+$ OLs are observed after P5 infections. Results in ***A*** are indicated as averages of proportions ± SEMs (E15, P5 $n = 3$; P1 $n = 5$). DCN, Deep cerebellar nuclei. Scale bars, 20 μm.

portion of interneurons (defined by means of morphological criteria and marker expression; Fig. 6) among GFP$^+$ cells decreased over time, in line with data obtained in GLAST::CreER^{T2}×R26R transgenic mice. Infected embryonic progenitors gave rise to all the variety of cerebellar interneurons, including Pax2$^+$ Golgi cells (Fig. 6*C*, arrow), Lugaro cells of the GL (data not shown; Fig. 6*A*), NeuN$^+$ deep cerebellar nuclei interneurons (data not shown; Fig. 6*A*), and PV$^+$ interneurons in the ML (Fig. 6*A*,*D*,*E*). Interneurons of the GL and those close to the PCL were still generated by LCMV-injected P1 progenitors (Fig. 6*A*,*I*, arrowheads in *J*), whereas they were virtually absent in the progeny of cells infected at P5 (Fig. 6*A*). At this latter stage, almost all GFP$^+$ interneurons resided in the most superficial part of the ML (Fig. 6*M*, arrows). These results recapitulate the physiological spatiotemporal pattern of interneuron specification (Leto et al., 2006, 2009).

Intriguingly, also the phenotypic repertoire of glial types produced at distinct time points differed during development. After LCMV infection in the embryo, we found a fraction of OL cells (identified as NG2$^+$/Olig2$^+$) in the cortical layers (Fig. 6*F*, arrows) or in the WM (Fig. 6*G*, arrows). However, after birth, the number of GFP$^+$ OLs dropped drastically (Fig. 6*A*,*O*). Conversely, the generation of parenchymal astrocytes (defined by means of morphological criteria and marker expression) in-

creased significantly over time and, when the PWM was targeted, for the most part included WM astrocytes (Fig. 6*A*, cfr with *H*, *K*, *N*). However, contrary to the other astrocytes, GFP-expressing BG derived primarily from embryonic and very early postnatal progenitors (P1) and not from PWM precursors at later developmental stages (Fig. 6*A*, arrowheads in *H*, *L*). Of note, in P5 injected animals, we found exclusively GFP$^+$ BG in proximity of the injection site, suggesting a direct infection of these cells rather than an origin from PWM progenitors. This pattern of BG generation is different from that of GLAST::CreER^{T2}×R26R mice in which BG cells accounted for a vast proportion of reporter-expressing cells after postnatal Tx administration (see above). This is arguably explained by direct recombination of immature BGs in the PCL.

On the whole, fate-mapping analyses demonstrated that LCMV-infected progenitors are able to generate astrocytes and interneurons during embryonic and early postnatal development, although to different extents.

In vitro and *in vivo* clonal analyses of PWM postnatal progenitors reveal their bipotency

Our data show that, at both embryonic and postnatal ages, interneurons are generated by primary precursors with astroglial traits. The same type of precursors also gives rise to mature parenchymal astrocytes. Nevertheless, it remains to be clarified whether a single progenitor is actually bipotent and produces both astrocytes and interneurons. To clarify this point, we focused on postnatal stages when the bulk of interneurogenesis occurs (Weisheit et al., 2006) and first performed *in vitro* clonal analyses. Cells isolated from the cerebellar PWM of P3 wild-type mice were plated at clonal density and cultured in serum-free condition with growth factors, as described previously (Qian et al., 2000; Kusek et al., 2012). After 4 d, we fixed the cells and evaluated the composition of the clones by colabeling for different lineage markers (BLBP for astroglial cells, Tuj1 for neurons; Fig. 7*A–E*). The majority of clones were composed of astrocytes (Fig. 7*A–F*). Furthermore, we found neuronal clones, and, interestingly, a consistent proportion of mixed clones, including both astrocytes and neurons (Fig. 7*C–F*). Neurons in the mixed clones belonged to the GFP$^+$ interneurons in Pax2–GFP-derived cultures (Fig. 7*D*). These mixed clones did not include OLs, despite the fact that isolated OLs or OL duplets were found in the cultures (data not shown). To further ensure that clones were originated from a single precursor, we mixed cells derived from P3 wild-type and β-actin–GFP PWM (Fig. 7*F*). We never observed clones composed of GFP-negative and GFP$^+$ cells, in agreement with their derivation from isolated single elements (data not shown). Moreover, we performed the same *in vitro* experiments by dissociating PWM cells from GLAST::CreER^{T2}×R26R^{YFP} mice that were induced *in vivo* with Tx 12 h before dissection. As above, plated cells included both reporter-positive and -negative elements. Also, this approach confirmed clonality and bipotency of PWM precursors (Fig. 7*E*,*F*). These *in vitro* data (listed in Fig. 7*F*) indicate that cerebellar progenitors can produce neurons and astrocytes in defined conditions and that these two lineages are strictly linked.

However, *in vitro* conditions may modify the *in vivo* differentiation potential of cells. Thus, we moved to the more physiological setting of organotypic cultures (DuPont et al., 2006; De Luca et al., 2015) and exploited the modified ubiquitous *StarTrack* (García-Marqués and López-Mascaraque, 2013) that (1) drives genomic integration of transgenes and (2) provides a unique combinatorial expression of different fluorescent proteins, allowing *in vivo* tracing of single cells and their progeny so to identify clones. To achieve this goal, we coelectroporated the ubiquitous *StarTrack* plasmid mix, encoding different fluorescent reporters along with the transposase plasmid. We performed *ex vivo* electroporation of P0–P2 cerebella and cultured organotypic slices for 7 d (Fig. 7*G*). We found a total of 35 different fluorescent combinations, and most of them (24) occurred only once with a frequency of 0.0179 (calculated as indicated by García-Marqués and López-Mascaraque, 2013). The complex range of color composition and the frequency of accuracy of each fluorescent mark confirmed the low probability for two different cells to acquire the same color code, corroborating the strength of this tool in our system. In five experiments, we analyzed 56 different clones. We found a vast predominance of astroglial clones, in line with the astroglial reactivity elicited by this culturing method (Dusart et al., 1997). However, four clones were identified as mixed clones, including interneurons and astrocytes. Figure 7*H* shows an example of a mixed clone composed by one immature interneuron identified by Pax2 expression (Fig. 7*H*) and cells with an immature astroglial phenotype.

As a third independent approach to address multipotency of PWM progenitors, we used the recently developed Confetti reporter mice (R26R^{Confetti}; Snippert et al., 2010) that enables us to distinguish clones derived from different single progenitor by means of the stochastic and exclusive expression of one of four fluorescent proteins (cytoplasmic yellow YFP or red RFP, membrane blue cyan fluorescent protein, and nuclear green GFP). We crossed R26R^{Confetti} with GLAST::CreER^{T2} and induced them at P3 with a low dose of Tx to induce recombination in only few and sparse astroglial-like progenitors. We first confirmed that 2 dpi recombined cells displayed an astroglial-like morphology and did not express the interneuron marker Pax2 (data not shown). We then analyzed at P30 the entire cerebella and mapped single cells, independently considering each color. This strategy yielded a small number of labeled cells per cerebellum (from ~10 to ~160 cells per fluorophore). The majority of labeled cells were BG and GL astrocytes that were excluded from this analysis because, at the examined time points, they predominantly derive from sources different from the neurogenic PWM, as demonstrated above. Accordingly, in cerebella containing only BG and GL astrocytes, no labeled interneurons were observed (two of seven cerebella), whereas the presence of tagged interneurons was always accompanied by color-matched WM astrocytes. In these cases, astrocytes were found either within the WM of a single lobule (intralobular WM; Fig. 7*I*) or in the WM at the bases of two adjacent lobules (Fig. 7*J*). In most cases, in the same section, a color-matched interneuron was observed in the ML of the same lobule or in that of one of the two abutting lobules in accordance with distinct astrocyte locations (Fig. 7*I*). Analysis of serial sections further revealed the presence of additional sister interneurons. Isolated color-matched interneurons in lobules unrelated to that containing WM astrocytes were never found. On these bases, we detected 15 mixed clones containing for the 73% at least two interneurons (3.7 ± 2.5 interneurons per clone), consistent with an intermediate amplification phase. Ninety-three percent of the same clones included one or two astrocytes (Fig. 7*I*, cells 1 and 2 of RFP clone), suggesting a very limited expansion along this lineage. The mean distance along the laterolateral axis of cells belonging to the same mixed clone was rather variable and had a median value of 550 μm, in line with the prominent migratory activity of interneurons along the cerebellar folia (Zhang and Goldman, 1996). In addition, in these animals, we found one and seven single clones composed exclusively of interneurons or WM astrocytes, respectively. No OLs or granule cells were targeted.

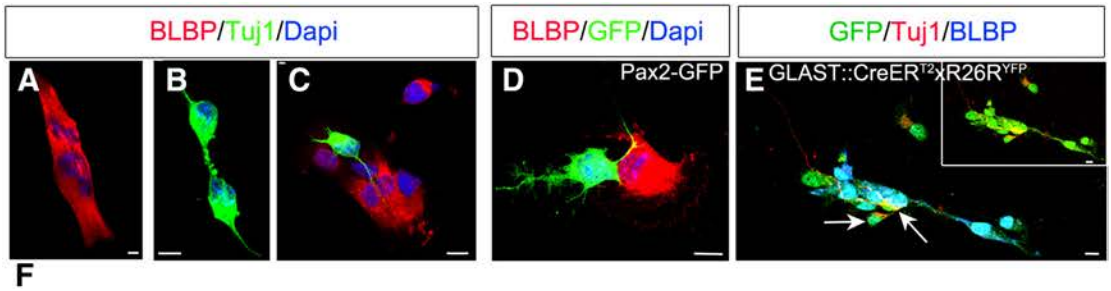

F

Experiments	N. experiments	Tot. clones analysed	Medium clones size (±SEM or dev st)	% glial clones (±SEM or dev st)	% neuronal clones (±SEM or dev st)	% mixed clones (±SEM or dev st)
wt	3	545	3.04 ± 0.15	86 ± 3%	3 ± 1,5%	11 ± 4.1%
βactin-GFP	2	228	3.07 ± 0.01	90.9 ± 0.4%	4.1 ± 1.7%	5 ± 2.1 %
GlastCreER^{T2}xR26R^{YFP}	3	639	3.5 ± 0.2	76.7 ± 2.7%	14.9 ± 1.3%	6.5 ± 2.9%

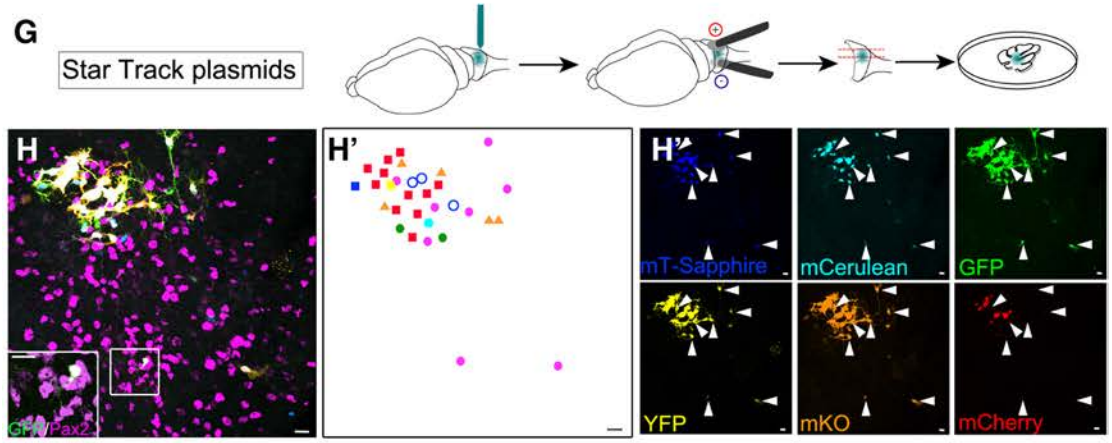

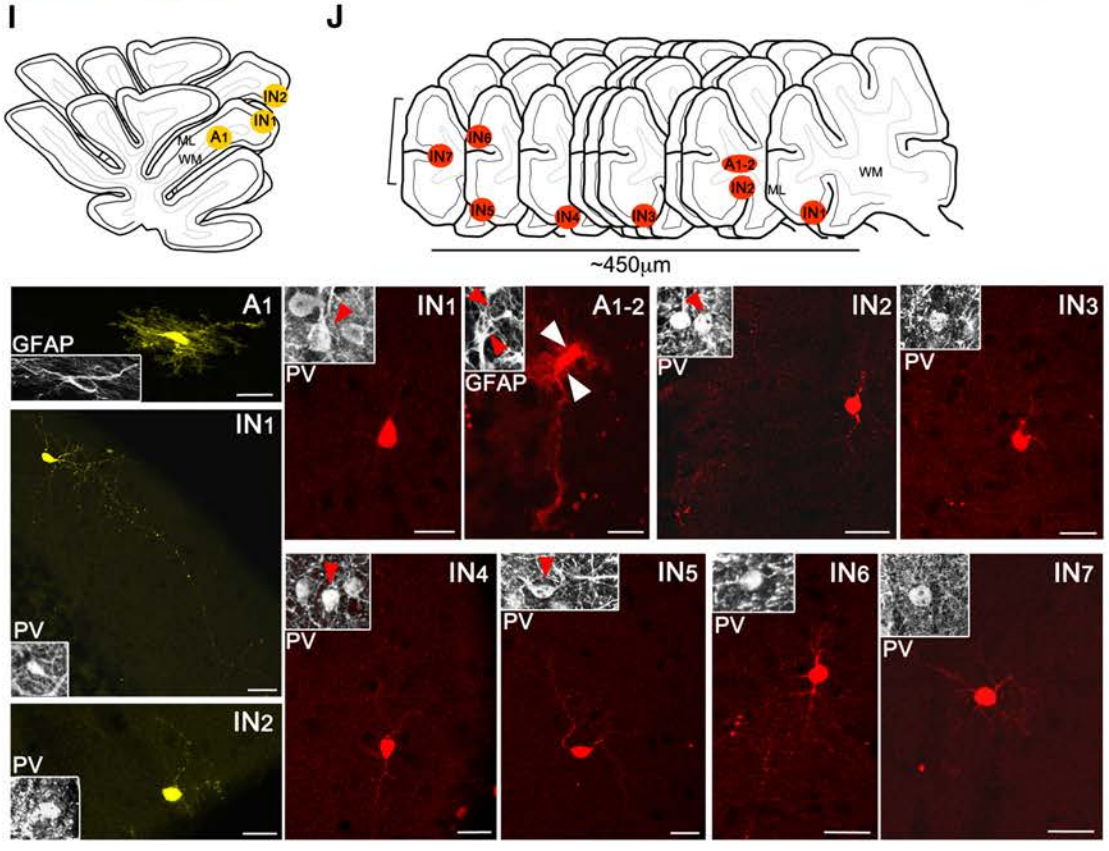

On the whole, these data are consistent with the existence in the postnatal cerebellum of a bipotent progenitor with astroglial features generating both interneurons and WM astrocytes.

Discussion

Proliferation and differentiation analyses of the PCL and PWM revealed that progenitors populating both niches display similar astroglial-like neurochemical profiles and exhibit different proliferative rates and progenies. Furthermore, PCL progenitors are highly proliferative, and they exclusively generate astroglia, mostly comprising BG cells. Conversely, PWM progenitors proliferate less frequently and produce both GABAergic interneurons and WM astrocytes. In addition, clonal analyses demonstrate the existence of bipotent PWM progenitors originating both inhibitory interneurons and astroglia of the WM.

Distinct proliferative activities of PCL and PWM niches

We show that different G_1-phase cyclin D proteins, known to positively regulate the cell cycle progression, are expressed in the PCL and PWM niches. Diverse cyclins are found in distinct neural progenitor populations in the developing telencephalon (Glickstein et al., 2007) and spinal cord (Lukaszewicz and Anderson, 2011), as well as in the adult hippocampus (Matsumoto et al., 2011). At these sites, they diversely regulate proliferation rates or neurogenesis of progenitor subsets, yet the specific effect of each isoform is not univocal but rather appears cell context dependent. In the cerebellum, while PCL progenitors express cD1, cD2 is found in the PWM. This differential expression is associated with a higher proliferative activity and a faster cell cycle reentry of PCL progenitors compared with PWM precursors. Consistent with a specific role in cell proliferation in the PWM, loss of cD2 dampens proliferation at this site but leaves that of the PCL unaffected. This suggests that these diverse cyclins may account specifically for the distinct proliferative rates of the PCL and PWM. In turn, diverse proliferation rhythms may also influence the differentiation properties of progenitors at these sites. Indeed, according to the "cell cycle length hypothesis," fast proliferation correlates with self-renewing divisions, whereas longer cell cycles favor neurogenic differentiation (Salomoni and Calegari, 2010). This could fit with what we observed in the postnatal cerebellum, in which fast divisions amplify self-renewing progenitors, ultimately producing BG in the PCL, whereas longer cell cycles associate with the production of interneurons by PWM cells (see also below). Moreover and in line with this view, loss of cD2 affects the proliferative rate of PWM cells and results in a reduction of the final number of cerebellar interneurons (Leto et al., 2011).

More active proliferation at the PCL compared with the PWM could also reflect the diverse expansion needs of progenitor cells in different cerebellar territories. Intense proliferation at the PCL leading to tangential amplification of prospective BG may be required to cope with the expansion of the cerebellar surface during postnatal foliation (Sudarov et al., 2007; Li et al., 2014), whereas more sporadic cell divisions may be sufficient to supply the adequate amount of interneurons.

Lineage of astroglial-like precursors and distinct progenies of PCL and PWM niches

Fate mapping in GLAST::CreER^{T2} mice and lentiviral-mediated analyses show that astroglial-like progenitors generate glial cells and interneurons in the embryonic and postnatal cerebellum. At earlier developmental ages, the full repertoire of interneurons and glial cells, including parenchymal astrocytes, BG, and OLs, is produced. Conversely, after P1, OLs disappear from the progeny of astroglial-like progenitors, as confirmed by the absence of GLAST-tagged mixed clones, including OLs both *in vitro* and *in vivo*. These data may suggest the existence of a multipotent progenitor that disappears as development proceeds. Nevertheless, previous studies pointed to an extracerebellar source for cerebellar OLs (Grimaldi et al., 2009; Mecklenburg et al., 2011). Previous data can be reconciled with the present results by the existence of an extracerebellar OL progenitor with astroglial traits that likely localize periventricularly, as required to be infected by intraventricular viral injections. However, after birth, astroglial-like OL progenitors appear exhausted, indicating a clear divergence of the OL lineage from that of postnatal cerebellar astroglial-like progenitors.

Notably, interneuron generation from fate-mapped progenitors occurs according to the formerly established sequence of interneuron specification, with earliest-born interneurons located deeper and later-born elements in more superficial positions (Leto et al., 2006, 2009). Thus, throughout cerebellar development, the capability to produce GABAergic neurons is maintained in a lineage of progenitors displaying features of primary astroglial-like precursors. These data confirm and extend previous results obtained in other mouse mutants in which progenitors of interneurons were shown to display astroglial traits, such as activity of the hGFAP promoter (Silbereis et al., 2009) and some degree of TenascinC expression (Fleming et al., 2013). Production of neurons from astroglial-like progenitors appears to decrease at the end of the first postnatal week, in line with previous studies (Silbereis et al., 2009). So far, reactivation of neurogenesis *in vivo* after this stage has not been reported (Grimaldi and Rossi, 2006; Su et al., 2014), despite successful isolation of adult cerebellar cells with NSC features and *in vitro* multipotency (Klein et al., 2005; Lee et al., 2005).

Lineage-tracing studies including ours fate mapped a population of cells without discriminating the exact spatial location of the neurogenic source. By *in vivo* selective genetic or viral-mediated targeting of either PCL or PWM progenitors, we fully clarify that only those in the PWM are neurogenic. Thus, the PWM hosts primary astroglial-like progenitors of GABAergic interneurons. Conversely, PCL progenitors exclusively generate other astrocytes. Of note, a distinct differentiation potential for PCL and PWM cells also emerges over time in regard to the astroglial progeny. Indeed, whereas PCL cells predominantly generate BG, PWM progenitors contribute to WM astrocytes.

←

Figure 7. Clonal analyses of postnatal cerebellar progenitors. ***A–F***, *In vitro* clonal analysis of cells isolated from the postnatal PWM of wild-type (***A–C***), Pax2–GFP (***D***), or GLAST::CreER^{T2}×R26R^{YFP} (***E***) mice. ***A***, BLBP$^+$ astroglial clone. ***B***, Tuj1$^+$ neuronal clone. ***C–E***, Mixed clones composed of astrocytes and neuron(s) (arrows in ***E***). ***F***, Summary of the *in vitro* experiments highlighting the total amount of analyzed clones. ***G***, Experimental procedure of *ex vivo* electroporations with a ubiquitous *StarTrack*. Representative example of mixed clones (***H***) with schematic representation of distinct color-coded clones (***H′***) and corresponding single channels (***H″***). Box in ***H*** shows a magnified Pax2$^+$ interneuron. Purple circles in the scheme and arrowheads in the single-channel pictures point to the identified mixed clone. ***I***, ***J***, *In vivo* clonal analysis of GLAST::CreER^{T2}×R26R^{Confetti} mice induced with a low dose of Tx and analyzed at P30. Representative two mixed clones composed of both WM astrocytes (A1, A2) and ML interneuron(s) (IN1–IN7; YFP and RFP) and their localization in serial parasagittal sections. The YFP$^+$ clone (***I***) comprises one WM astrocyte and two interneurons located in the same lobule of contiguous sections, whereas the RFP$^+$ clone (***J***) is composed of two astrocytes (arrowheads) in the WM and seven sister interneurons in the above lobules. Insets show GFAP or PV expression of the fluorescent cells. Scale bars: ***A–E***, 10 μm; ***H–J***, 20 μm.

These data implicate diverse functions for NSC-related genes found in both PCL and PWM (Alcock et al., 2009; Silbereis et al., 2009; Fleming et al., 2013). This may be attributable to the cooperation with other undefined intrinsic factors and/or to the influence of environmental cues. Moreover, they underline a functional divergence of the PCL/PWM progenitor pools that fits well the classical view of a distinct ontogenesis. Indeed, whereas PCL progenitors are posited to derive directly from RG through the retraction of apical processes, PWM progenitors are instead postulated to emigrate from the VZ apparently without any basal or apical anchor (Buffo and Rossi, 2013 and references therein). Of note, the occurrence of these processes still awaits a direct demonstration.

Bipotent progenitors in the PWM produce both interneurons and WM astrocytes

The consistent and parallel production of both interneurons and astroglia from astroglial-like progenitors raises the issue of the existence of bipotent progenitors. Previous studies suggested a lineage relationship between astrocytes and GABAergic interneurons (Silbereis et al., 2009; Sudarov et al., 2011). More recently, it was proposed that postnatal CD15$^+$-intermediate progenitors for astrocytes and Ptf1a$^+$-intermediate progenitors for interneurons derive from common CD133$^+$ precursors, thus implicating a lineage relationship between these two cell populations (Fleming et al., 2013). Our clonal analyses provide the first *in vitro* and *in vivo* evidence for the existence of bipotent astroglial-like PWM progenitors producing both interneurons and WM astrocytes. *In vitro* analyses show a small but consistent fraction (~7%) of clones composed of both astrocytes and interneurons. More importantly, our *in vitro* data are corroborated by evidence of mixed clones *in vivo*. Targeting single progenitors by low Tx doses in GLAST::CreER^{T2}×R26R^{Confetti} mice produces a progeny formed by color-matched WM astrocytes and ML interneurons that we define as clones based on the following observations: (1) shortly after low-dose Tx treatment, no recombination in Pax2$^+$ interneurons was found, thereby excluding the possibility of a direct targeting of these cells; (2) animals in which no WM astrocytes are tagged lacked interneurons; (3) in most cases, interneurons and astrocytes displayed clear spatial association being found in the same lobule; and (4) interneuron clones without WM astrocytes were extremely rare. Cerebellar interneuron clusters produced postnatally are dispersed broadly laterolaterally (from ~100 to ~750 μm) and from the sister astrocytes (from ~0 to ~200 μm) but consistently found in the same lobules, according with the striking migratory capability of interneurons in the ML (Zhang and Goldman, 1996; Cameron et al., 2009) and with the neuroanatomical organization of the cerebellum (Sillitoe and Joyner, 2007).

At difference with the well defined clonal relationships between RG-derived astrocytes and glutamatergic neurons in the neocortex (Magavi et al., 2012; Guo et al., 2013; Gao et al., 2014), few studies addressed the lineage link between interneurons and astrocytes in the nervous system. However, a common derivation of astrocytes and subpallium-derived neocortical interneurons has been suggested recently (Magavi et al., 2012). Similar to our findings, this study shows that, although interneurons migrate far away from their site of origin, sister astrocytes remain nearby and colonize the striatum during both the embryonic and early postnatal cortical development (Magavi et al., 2012; Tsai et al., 2012). Thus, broad displacement of sister cells may be a common feature of interneuron–astroglial clones. On the whole, these clonal analyses point to the existence of bipotent progenitors in the postnatal cerebellum. Examining whether such progenitors also exist at earlier developmental ages and, if so, what neuron and companion astroglia populations they might contribute will be of particular interest in the future.

References

Alcock J, Sottile V (2009) Dynamic distribution and stem cell characteristics of Sox1-expressing cells in the cerebellar cortex. Cell Res 19:1324–1333. CrossRef Medline

Alcock J, Scotting P, Sottile V (2007) Bergmann glia as putative stem cells of the mature cerebellum. Med Hypotheses 69:341–345. CrossRef Medline

Altman J, Bayer SA (1997) Development of cerebellar system in relation to its evolution, structure and functions. Boca Raton, FL: CRC.

Alvarez Otero R, Sotelo C, Alvarado-Mallart RM (1993) Chick/quail chimeras with partial cerebellar grafts: an analysis of the origin and migration of cerebellar cells. J Comp Neurol 333:597–615. CrossRef Medline

Anthony TE, Klein C, Fishell G, Heintz N (2004) Radial glia serve as neuronal progenitors in all regions of the central nervous system. Neuron 41: 881–890. CrossRef Medline

Anthony TE, Mason HA, Gridley T, Fishell G, Heintz N (2005) Brain lipid-binding protein is a direct target of Notch signaling in radial glial cells. Genes Dev 19:1028–1033. CrossRef Medline

Bastianelli E (2003) Distribution of calcium-binding proteins in the cerebellum. Cerebellum 2:242–262. CrossRef Medline

Bi B, Salmaso N, Komitova M, Simonini MV, Silbereis J, Cheng E, Kim J, Luft S, Ment LR, Horvath TL, Schwartz ML, Vaccarino FM (2011) Cortical glial fibrillary acidic protein-positive cells generate neurons after perinatal hypoxic injury. J Neurosci 31:9205–9221. CrossRef Medline

Bonaguidi MA, Wheeler MA, Shapiro JS, Stadel RP, Sun GJ, Ming GL, Song H (2011) In vivo clonal analysis reveals self-renewing and multipotent adult neural stem cell characteristics. Cell 145:1142–1155. CrossRef Medline

Buffo A, Rossi F (2013) Origin, lineage and function of cerebellar glia. Prog Neurobiol 109:42–63. CrossRef Medline

Buffo A, Rite I, Tripathi P, Lepier A, Colak D, Horn AP, Mori T, Götz M (2008) Origin and progeny of reactive gliosis: a source of multipotent cells in the injured brain. Proc Natl Acad Sci U S A 105:3581–3586. CrossRef Medline

Cameron DB, Kasai K, Jiang Y, Hu T, Saeki Y, Komuro H (2009) Four distinct phases of basket/stellate cell migration after entering their final destination (the molecular layer) in the developing cerebellum. Dev Biol 332:309–324. CrossRef Medline

Carletti B, Rossi F (2008) Neurogenesis in the cerebellum. Neuroscientist 14:91–100. CrossRef Medline

De la Rossa A, Bellone C, Golding B, Vitali I, Moss J, Toni N, Lüscher C, Jabaudon D (2013) In vivo reprogramming of circuit connectivity in postmitotic neocortical neurons. Nat Neurosci 16:193–200. CrossRef Medline

De Luca A, Parmigiani E, Tosatto G, Martire S, Hoshino M, Buffo A, Leto K, Rossi F (2015) Exogenous Sonic hedgehog modulates the pool of GABAergic interneurons during cerebellar development. Cerebellum 14: 72–85. CrossRef Medline

Dupont JL, Fourcaudot E, Beekenkamp H, Poulain B, Bossu JL (2006) Synaptic organization of the mouse cerebellar cortex in organotypic slice cultures. Cerebellum 5:243–256 CrossRef Medline

Dusart I, Airaksinen MS, Sotelo C (1997) Purkinje cell survival and axonal regeneration are age dependent: an in vitro study. J Neurosci 17:3710–3726. Medline

Fleming JT, He W, Hao C, Ketova T, Pan FC, Wright CCV, Litingtung Y, Chiang C (2013) The Purkinje neuron acts as a central regulator of spatially and functionally distinct cerebellar precursors. Dev Cell 27:278–292. CrossRef Medline

Gao P, Postiglione MP, Krieger TG, Hernandez L, Wang C, Han Z, Streicher C, Papusheva E, Insolera R, Chugh K, Kodish O, Huang K, Simons BD, Luo L, Hippenmeyer S, Shi SH (2014) Deterministic progenitor behavior and unitary production of neurons in the neocortex. Cell 159:775–788. CrossRef Medline

García-Marqués J, López-Mascaraque L (2013) Clonal identity determines astrocyte cortical heterogeneity. Cereb Cortex 23:1463–1472. Medline

Glickstein SB, Alexander S, Ross ME (2007) Differences in cyclin D2 and D1 protein expression distinguish forebrain progenitor subsets. Cereb Cortex 17:632–642. Medline

Grimaldi P, Rossi F (2006) Lack of neurogenesis in the adult rat cerebellum after Purkinje cell degeneration and growth factor infusion. Eur J Neurosci 23:2657–2668. CrossRef Medline

Grimaldi P, Parras C, Guillemot F, Rossi F, Wassef M (2009) Origins and control of the differentiation of inhibitory interneurons and glia in the cerebellum. Dev Biol 328:422–433. CrossRef Medline

Guo C, Eckler MJ, McKenna WL, McKinsey GL, Rubenstein JLR, Chen B (2013) Fezf2 expression identifies a multipotent progenitor for neocortical projection neurons, astrocytes, and oligodendrocytes. Neuron 80: 1167–1174. CrossRef Medline

Hallonet ME, Teillet MA, Le Douarin NM (1990) A new approach to the development of the cerebellum provided by the quail-chick marker system. Development 108:19–31. Medline

Klein C, Butt SJB, Machold RP, Johnson JE, Fishell G (2005) Cerebellum- and forebrain-derived stem cells possess intrinsic regional character. Development 132:4497–4508. CrossRef Medline

Kusek G, Campbell M, Doyle F, Tenenbaum SA, Kiebler M, Temple S (2012) Asymmetric segregation of the double-stranded RNA binding protein Staufen2 during mammalian neural stem cell divisions promotes lineage progression. Cell Stem Cell 11:505–516. CrossRef Medline

Lee A, Kessler JD, Read TA, Kaiser C, Corbeil D, Huttner WB, Johnson JE, Wechsler-Reya RJ (2005) Isolation of neural stem cells from the postnatal cerebellum. Nat Neurosci 8:723–729. CrossRef Medline

Leto K, Carletti B, Williams IM, Magrassi L, Rossi F (2006) Different types of cerebellar GABAergic interneurons originate from a common pool of multipotent progenitor cells. J Neurosci 26:11682–11694. CrossRef Medline

Leto K, Bartolini A, Yanagawa Y, Obata K, Magrassi L, Schilling K, Rossi F (2009) Laminar fate and phenotype specification of cerebellar GABAergic interneurons. J Neurosci 29:7079–7091. CrossRef Medline

Leto K, Bartolini A, Di Gregorio A, Imperiale D, De Luca A, Parmigiani E, Filipkowski RK, Kaczmarek L, Rossi F (2011) Modulation of cell-cycle dynamics is required to regulate the number of cerebellar GABAergic interneurons and their rhythm of maturation. Development 138:3463–3472. CrossRef Medline

Leto K, Rolando C, Rossi F (2012) The genesis of cerebellar GABAergic neurons: fate potential and specification mechanisms. Front Neuroanat 6:6. CrossRef Medline

Li K, Leung AW, Guo Q, Yang W, Li JYH (2014) Shp2-dependent ERK signaling is essential for induction of Bergmann glia and foliation of the cerebellum. J Neurosci 34:922–931. CrossRef Medline

Lukaszewicz AI, Anderson DJ (2011) Cyclin D1 promotes neurogenesis in the developing spinal cord in a cell cycle-independent manner. Proc Natl Acad Sci U S A 108:11632–11637. CrossRef Medline

Magavi S, Friedmann D, Banks G, Stolfi A, Lois C (2012) Coincident generation of pyramidal neurons and protoplasmic astrocytes in neocortical columns. J Neurosci 32:4762–4772. CrossRef Medline

Mathis L, Nicolas JF (2003) Progressive restriction of cell fates in relation to neuroepithelial cell mingling in the mouse cerebellum. Dev Biol 258:20–31. CrossRef Medline

Matsumoto Y, Tsunekawa Y, Nomura T, Suto F, Matsumata M, Tsuchiya S, Osumi N (2011) Differential proliferation rhythm of neural progenitor and oligodendrocyte precursor cells in the young adult hippocampus. PLoS One 6:e27628. CrossRef Medline

Mecklenburg N, Garcia-López R, Puelles E, Sotelo C, Martinez S (2011) Cerebellar oligodendroglial cells have a mesencephalic origin. Glia 59: 1946–1957. CrossRef Medline

Milosevic A, Goldman JE (2004) Potential of progenitors from postnatal cerebellar neuroepithelium and white matter: lineage specified vs. multipotent fate. Mol Cell Neurosci 26:342–353. CrossRef Medline

Mori T, Tanaka K, Buffo A, Wurst W, Kühn R, Götz M (2006) Inducible gene deletion in astroglia and radial glia—a valuable tool for functional and lineage analysis generation of mice. Glia 54:21–34. CrossRef Medline

Okabe M, Ikawa M, Kominami K, Nakanishi T, Nishimune Y (1997) "Green mice" as a source of ubiquitous green cells. FEBS Lett 407:313–319. CrossRef Medline

Pevny LH, Nicolis SK (2010) Sox2 roles in neural stem cells. Int J Biochem Cell Biol 42:421–424. CrossRef Medline

Pfeffer PL, Payer B, Reim G, di Magliano MP, Busslinger M (2002) The activation and maintenance of Pax2 expression at the mid-hindbrain boundary is controlled by separate enhancers. Development 129:307–318. Medline

Qian X, Shen Q, Goderie SK, He W, Capela A, Davis AA, Temple S (2000) Timing of CNS cell generation: a programmed sequence of neuron and glial cell production from isolated murine cortical stem cells. Neuron 28:69–80. CrossRef Medline

Salomoni P, Calegari F (2010) Cell cycle control of mammalian neural stem cells: putting a speed limit on G1. Trends Cell Biol 20:233–243. CrossRef Medline

Sherr CJ (1995) Mammalian G1 cyclins and cell cycle progression. Proc Assoc Am Physicians 107:181–186. Medline

Sherr CJ, Roberts JM (1999) CDK inhibitors: positive and negative regulators of G1-phase progression. Genes Dev 13:1501–1512. CrossRef Medline

Sicinski P, Donaher JL, Geng Y, Parker SB, Gardner H, Park MY, Robker RL, Richards JS, McGinnis LK, Biggers JD, Eppig JJ, Bronson RT, Elledge SJ, Weinberg RA (1996) Cyclin D2 is an FSH-responsive gene involved in gonadal cell proliferation and oncogenesis. Nature 384:470–474. CrossRef Medline

Silbereis J, Cheng E, Ganat YM, Ment LR, Vaccarino FM (2009) Precursors with glial fibrillary acidic protein promoter activity transiently generate GABA interneurons in the postnatal cerebellum. Stem Cells 27:1152–1163. CrossRef Medline

Sillitoe RV, Joyner AL (2007) Morphology, molecular codes, and circuitry produce the three-dimensional complexity of the cerebellum. Annu Rev Cell Dev Biol 23:549–577. CrossRef Medline

Simat M, Ambrosetti L, Lardi-Studler B, Fritschy JM (2007) GABAergic synaptogenesis marks the onset of differentiation of basket and stellate cells in mouse cerebellum. Eur J Neurosci 26:2239–2256. CrossRef Medline

Snippert HJ, van der Flier LG, Sato T, van Es JH, van den Born M, Kroon-Veenboer C, Barker N, Klein AM, van Rheenen J, Simons BD, Clevers H (2010) Intestinal crypt homeostasis results from neutral competition between symmetrically dividing Lgr5 stem cells. Cell 143:134–144. CrossRef Medline

Soriano P (1999) Generalized lacZ expression with the ROSA26 Cre reporter strain. Nat Genet 21:70–71. CrossRef Medline

Srinivas S, Watanabe T, Lin CS, William CM, Tanabe Y, Jessell TM, Costantini F (2001) Cre reporter strains produced by targeted insertion of EYFP and ECFP into the ROSA26 locus. BMC Dev Biol 1:4. CrossRef Medline

Stein CS, Martins I, Davidson BL (2005) The lymphocytic choriomeningitis virus envelope glycoprotein targets lentiviral gene transfer vector to neural progenitors in the murine brain. Mol Ther 11:382–389. CrossRef Medline

Su X, Guan W, Yu YC, Fu Y (2014) Cerebellar stem cells do not produce neurons and astrocytes in adult mouse. Biochem Biophys Res Commun 450:378–383. CrossRef Medline

Sudarov A, Joyner AL (2007) Cerebellum morphogenesis: the foliation pattern is orchestrated by multi-cellular anchoring centers. Neural Dev 2:26. CrossRef Medline

Sudarov A, Turnbull RK, Kim EJ, Lebel-Potter M, Guillemot F, Joyner AL (2011) Ascl1 genetics reveals insights into cerebellum local circuit assembly. J Neurosci 31:11055–11069. CrossRef Medline

Tsai HH, Li H, Fuentealba LC, Molofsky AV, Taveira-Marques R, Zhuang H, Tenney A, Murnen AT, Fancy SPJ, Merkle F, Kessaris N, Alvarez-Buylla A, Richardson WD, Rowitch DH (2012) Regional astrocyte allocation regulates CNS synaptogenesis and repair. Science 337:358–362. CrossRef Medline

Weisheit G, Gliem M, Endl E, Pfeffer PL, Busslinger M, Schilling K (2006) Postnatal development of the murine cerebellar cortex: formation and early dispersal of basket, stellate and Golgi neurons. Eur J Neurosci 24: 466–478. CrossRef Medline

Yamada K, Watanabe M (2002) Cytodifferentiation of Bergmann glia and its relationship with Purkinje cells. Anat Sci Int 77:94–108. CrossRef Medline

Zhang L, Goldman JE (1996) Developmental fates and migratory pathways of dividing progenitors in the postnatal rat cerebellum. J Comp Neurol 370:536–550. CrossRef Medline